AD-A044 858 ILLINOIS UNIV AT URBANA-CHAMPAIGN DEPT OF CIVIL ENGIN--ETC F/G 13/5
EFFECTS OF LACK-OF-PENETRATION AND LACK-OF-FUSION ON THE FATIGU--ETC(U)
JUL 76 J D BURK, F V LAWRENCE N00024-75-C-4504

UNCLASSIFIED NL

1 OF 1
ADA
044858

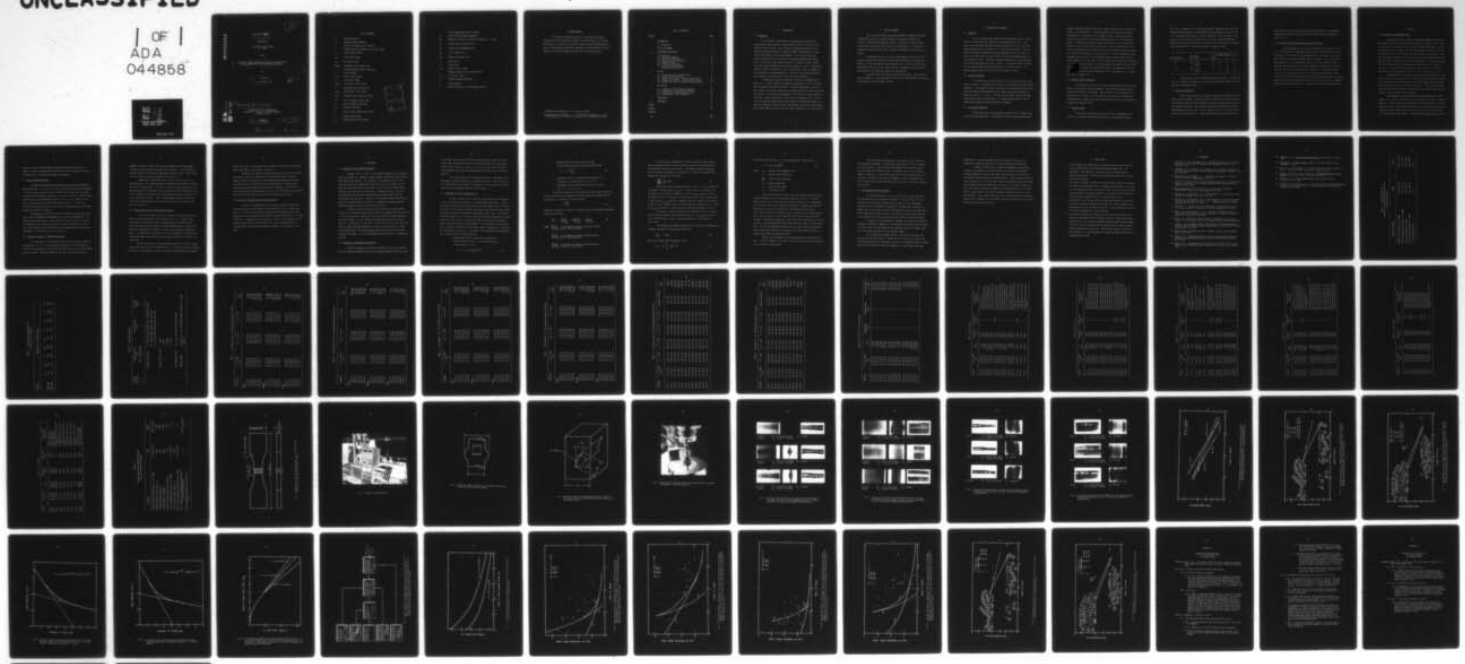

END
DATE
FILMED
10-77
DDC

9 MRC

(9) FINAL REPORT,

Submitted to

Naval Sea Systems Command
U. S. Navy

on the

(6) EFFECTS OF LACK-OF-PENETRATION AND LACK-OF-FUSION ON THE FATIGUE PROPERTIES OF 5083 ALUMINUM ALLOY WELDS

by

(10) J. D. Burk
F. V. Lawrence, Jr

(15) N00024-75-C-4504

Department of Civil Engineering
University of Illinois at Urbana-Champaign
Urbana, Illinois

(11) July 1976

(12) 70 p.

176 010

LIST OF SYMBOLS

a	Material constant
b	Fatigue strength exponent
β	Angle of inclination for LOF defect
c	Fatigue ductility exponent; also, crack length
c_o	Initial crack length
c_f	Final crack length
$2c_o$	LOP defect width
dc/dN	Incremental crack growth rate
C	Crack propagation material constant
E	Elastic modulus
$e, \Delta e$	Nominal strain, range
$\varepsilon, \Delta\varepsilon$	True strain, range
$\varepsilon_e, \Delta\varepsilon_e$	True elastic strain, range
ε_f'	Fatigue ductility coefficient
$\varepsilon_p, \Delta\varepsilon_p$	True plastic strain, range
ΔK_{th}	Threshold stress intensity factor
ΔK	Stress intensity factor range
K'	Cyclic strength coefficient
K_f	Fatigue notch factor
K_t	Elastic stress concentration factor
ℓ	Length of LOF defect
ℓ_o	Projected width of LOF defect

n	Crack propagation material constant
n'	Cyclic strain hardening exponent
$2N_f$	Number of reversals to failure (2 reversals = 1 cycle)
N_I	Fatigue crack initiation life
N_p	Fatigue crack propagation life
N_T	Total fatigue life
$2N_t$	Transition fatigue life
r	Notch radius
R	Stress ratio
$S, \Delta S$	Nominal stress, range
s	Minimum distance of LOF defect from surface
$\sigma, \Delta\sigma$	True stress, range
σ'_f	Fatigue strength coefficient
t	Plate thickness
w	Width of the weld at reinforcement position

ACKNOWLEDGEMENTS

This study was sponsored by the U.S. Navy Naval Sea Systems Command under Contract N00024-75-C-4504. The authors would like to thank the sponsor; Mr. Tom West, the technical monitor; and the Welding Research Council Aluminum Alloys Committee*, Subcommittee on Weld Defects** for their support and interest throughout the duration of the investigation.

* Aluminum Alloys Committee: R. A. Kelsey, Chairman

** Subcommittee on Weld Defects: L. J. Christensen, Chairman; D. C. Hill; W. B. Jenkins; W. J. Louis; R. D. Merrick; G. R. Rothschild; W. Wong.

TABLE OF CONTENTS

1. INTRODUCTION

1.1 Background

The influence of weld defects on the mechanical properties of constructional grade aluminum alloy weldments has been the subject of considerable recent interest. The influence of distributed porosity on the tensile and fatigue properties of 5083 (and 6061) alloy weldments has been recently investigated by the authors ~~(1,2)~~. In the fatigue study ~~(2)~~, defects other than the weld toe and/or distributed porosity (most notably lack-of-fusion) were often found to result in substantially lower fatigue lives than would be expected from sound, as-welded test pieces. Consequently internal, planar, weld-defects such as lack-of-fusion (LOF) or incomplete joint penetration (lack-of-penetration - LOP) must be considered potentially serious defects from the point of view of fatigue resistance.

Dinsdale and Young (3) studied the influence of "double operator defects" i.e., lack-of-fusion and incomplete penetration in 1/2-in. (12.7-mm) thick Al-Mg-Mn alloys (NP 5/6 and NP 8). The exact dimensions of the LOP in their study is not clearly stated, but the defects apparently persisted for the full length of the weld and were between 14 to 25 percent of the thickness of the joints, rather large defects by current U.S.N. standards (4,5). The result of Dinsdale and Young's work clearly shows that LOP and LOF defects can reduce the fatigue resistance of both reinforcement intact (RI) and reinforcement removed (RR) test pieces below the normal expectations for sound RI welds.

2. SCOPE OF PROGRAM

Zero to tension fatigue tests were performed on double-V butt welds of 5083/5183 aluminum alloy which contained full-length LOP defects and "natural", less-than-full-length LOF defects. The LOP and LOF defects were incorporated in the welds using "improper" welding methods. The defects so created were evaluated using normal incidence radiography and ultrasonic test methods.

Fatigue tests were run on sound reinforcement intact (RI) and reinforcement removed (RR) welds and RI and RR welds containing full-length LOP defects of various through thickness dimensions (2c). Fatigue tests were run on RR welds containing various length "natural" LOF defects in order to study the behavior of less-than-full length, inclined defects.

The total fatigue lives were predicted analytically. The effectiveness of current U.S. Navy radiographic and ultrasonic test methods were examined in the light of the experimental results.

3. EXPERIMENTAL PROCEDURES

3.1 Materials

The test specimens were machined from welded panels 24-in. (61-cm) by 36-in. (92-cm) which were donated by Chicago Bridge and Iron Co. The panels were fabricated from 5083 aluminum base metal using a 5183 wire electrode and were 3/8-in. (9.6-mm) and 1-in. (25.4-mm) in thickness. The base metal-filler metal combination and plate thicknesses used in this work are the same as those used in previous studies of welds and 5083/5183 welds containing porosity (2,6). The nominal mechanical properties of the plate material and 5183 weld metal are given in Table 1. The typical chemical composition of 5083 base metal and 5183 weld metal are listed in Table 2. The specimen nomenclature used in the study is outlined in Table 3.

3.2 Welding Procedures

All welded panels were fabricated in the flat position using a gas-metal-arc process. Sound weld panels (level 1), were welded using conventional procedures. Three groups of panels were welded to intentionally produce small, medium and large lack-of-penetration (LOP) defects and were designated by severity as levels 2, 3, and 4. Lack-of-fusion weld panels containing intermittent defects were also fabricated. All panels were furnished in the as-welded state without any post-weld terminal treatment.

3.3 Test Piece Preparation

Fatigue test pieces were prepared by cutting 3 1/2-in. (89-mm) wide strips from the welded panels. Radiographs of panels containing LOP defects

showed a continuous defect while those of panels containing LOF indicated the defects to be intermittent. Lack-of-penetration test pieces were therefore continuously cut from one end of the supplied panels. Lack-of-fusion test pieces were selectively cut from the panels with the aid of the panel radiographs. A reduced cross-section having a gage length of 2-in. (51-mm) and width of 2-in. (51-mm) for LOP test pieces or 2 1/2-in. (64-mm) for LOF test pieces was machined into the strips. The LOF test pieces were wider to insure the inclusion of the defect in the test section. To avoid problems with test equipment, LOP test pieces to be fatigued at higher stress ranges had their width reduced to 1-in. (25.4-mm). All test pieces were either 3/8-in. (9.6-mm) or 1-in. (25-mm) in thickness. The reinforcement was removed from the LOF test pieces and approximately half the LOP test pieces. The remainder of the test pieces were tested with the reinforcement intact. The geometry for a typical test piece is shown in Fig. 1.

3.4 Non-Destructive Examination

After machining, all test pieces were examined and rated using radiographic and ultrasonic inspection methods. Edge shot radiographs were taken of both the LOP and LOF test pieces. Each test piece was ultrasonically inspected prior to testing. Prior to each test, the ultrasonic equipment was calibrated with a standard test block as described by the U.S. Navy inspection standard (see Appendix A) (4).

3.5 Fatigue Testing

The weld test pieces were tested to failure or approximately 10^7 cycles with a 50,000 lb MTS closed-loop hydraulic test apparatus (shown in

Fig. 2) at a frequency of 5 to 10 Hz under ambient laboratory conditions (20°C and 50% relative humidity). A 600,000 MTS testing apparatus was used for the 1-in. (25.4-mm) LOF test pieces. Zero-to-tension (R = 0), sinusoidal, stress cycles of 0 to 19 ksi (131.0 MPa) or 0 to 12 ksi (82.7 MPa) were employed. These stress ranges were selected on the basis of the previous work of Sanders and the authors (2,6). The testing program is summarized below:

Reinforcement	Thickness in.	(mm)	LOP Defect Level 1 (sound)	2	3	4
RI	3/8	(9.5)	12	6	6	6
	1	(25.4)	6	6	6	6
RR	3/8	(9.5)	--	6	6	6
	1	(25.4)	--	6	6	6

In addition to the tests tabulated above, twelve 3/8-in. (9.6-mm) and ten 1-in. (25.4-mm) test pieces, containing intermittent LOF defects with reinforcement removed (RR) tested.

3.6 Post-Test Examination

After fatigue testing, the fracture surfaces were examined, and the defect size was measured. The actual widths of the defects varied slightly on the fracture surface, and the measurement of width was complicated by porosity associated with the LOP. Lack-of-penetration width measurements were made at the maximum width of the defect on the fracture surface or at the location of crack initiation (see Fig. 3). Lack-of-fusion defects were inclined to the

fracture surface, and their widths were not readily measured. Approximate measurements of the LOF widths were made from the edge shot radiographs as shown in Fig. 4.

3.7 Low Cycle Fatigue Specimen Preparation and Testing

Smooth specimens for low cycle fatigue (LCF) testing were cut from a 1-in. (25.4-mm) thick sound 5083/5183 weld panel. Fatigue testing was conducted with an MTS 20,000 lb. closed-loop hydraulic test apparatus (7) with Wood's metal grips to ensure proper specimen alignment. Axial strains were measured with a clip-on extensometer (see Fig. 5) for the 5083 base metal specimens and calculated with an analog computer from measured load and diametrical strains for the 5183 weld metal specimens. A completely reversed ($R = -1$) sine wave was used to control specimen strain amplitude. Eight specimens of both 5083 base metal and 5183 weld metal were fatigued to failure under strain control to produce fatigue lives of 10^2 to 10^6 cycles. Monotonic tension tests were performed on one specimen each of the weld and base metal.

4. RESULTS

4.1 Description of LOP and LOF Flaws

The fracture surfaces, normal incidence radiographs, and edge shot radiographs of typical lack-of-penetration defects are shown in Figs. 6 and 7 for both 3/8-in. (9.6-mm) and 1-in. (25.4-mm) thickness specimens. The fracture surfaces in Figs. 6 and 7 show that large amounts of porosity are associated with the LOP. This porosity has been previously reported (3). There was considerable variation in the distribution of the porosity along the LOP defect as well as variation in the size of the porosity. The porosity shape also varied from spherical to elongated, worm-hole porosity. Examination of the fracture surfaces revealed that fatigue crack initiation occurred predominately from the LOP defect and was not associated with the porosity.

Representative lack-of-fusion fracture surfaces and edge shot radiographs are shown in Figs. 8 and 9. In contrast to the continuous LOP defects, the LOF defects were crescent-shaped, intermittent defects and their length was aligned with the axis of the weld: see Fig. 4. Unlike the LOP defects, porosity was not associated with the LOF defects; but a dark oxide layer was evident at the LOF defect internal surfaces.

The parameters used to characterize the LOP and LOF defects are shown in Figs. 3 and 4. Dimensions of the LOP defects are listed in Tables 4 through 7. Tables 8 and 9 give the dimensions of the LOF defects. The LOF defect width ($2c_o$) ranged from 0.002 to 0.18-in. (0.51 to 4.6-mm) for 3/8-in. (9.6-mm) thick test pieces and from 0.002 to 0.30-in. (0.51 to 7.6-mm) for 1-in. (25.4-mm) thick test pieces. The LOF defect projected width (ℓ_o) did

not vary as much as the LOP defect length ($2c_o$) and ranged from 0.05 to 0.08-in. (1.27 to 2.03-mm) and 0.08 to 0.30-in. (2.03 to 7.62-mm) for 3/8-in. (9.6-mm) and 1-in. (25.4-mm) test pieces, respectively.

4.2 Results of NDT Evaluation

All test pieces were rated ultrasonically using Navy code NAVSHIPS 0900-006-3010 (4); i.e., Class I, II, III, or rejection as outlined in Appendix A. Each test piece rating is given in Tables 10-16. Almost all test pieces containing LOP defects were rated Class I: *none were rejected.* The test pieces containing LOF were predominately rated as Class II or III. Several of the 3/8-in. (9.6-mm) thick test pieces were rated as Class I. The LOF 1-in. (25.4-mm) test pieces was the only group which contained test pieces that were rejected by ultrasonic inspection.

Radiographs of the LOP test pieces and sound test pieces were rated by U.S. Navy code NAVSHIPS 0900-003-9000 (5) as outlined in Appendix B. All sound welds received a Class I rating, and *all LOP test pieces were rejected.* The radiographs of LOP defects were similar to those shown in Figs. 6 and 7. Test pieces containing LOF defects were rated using the normal incidence panel radiographs. *All LOF test pieces were rejected.*

4.3 Fatigue Test Results: Sound RI Test Pieces

The test results for the sound RI test pieces are given in Table 10 and plotted in Fig. 10. A least-squares line shown solid in the figure was fitted to the open symbol test data for both the 3/8 and 1-in. (9.6 and 25.4-mm) thick test pieces. The solid symbols of the 3/8-in. (9.6-mm) test pieces

(numbers 1 though 6 in Table 10) were not considered in the least-squares fit because these specimens had large joint distortions. Such distortions have been shown to significantly reduce weld fatigue life (9). Results from a prior study (2) are shown as dashed lines in Fig. 10.

Comparison of the best-fit lines in Fig. 10 shows that the 1-in. (25.4-mm) welds in this study produced significantly better fatigue lives than the 3/8-in. (9.6-mm) welds. This result is opposite to that obtained in the previous work and is attributed to the fact that the weld reinforcement of the 3/8-in. (9.6-mm) test pieces of this study were much larger than that of the 1-in. (25.4-mm) test pieces. There is good agreement between the best-fit lines (solid and dashed) for the 1-in. (25.4-mm) test pieces for this study and the prior work.

4.4 Fatigue Test Results: LOP and LOF Test Pieces

The LOP test results for 3/8-in. (9.6-mm) test pieces are listed in Tables 5 and 6 and plotted in the S-N diagram of Fig. 11. The data show a large amount of scatter which results from differences in LOP width ($2c_o$). Those test pieces having the larger LOP widths produced shorter fatigue lives than those with smaller LOP defects. All but a few specimens failed at LOP defects. A comparison of the best-fit lines for sound welds to the welds containing LOP shows that the *LOP test pieces always produced lives shorter than sound welds.*

Results for the 1-in. (25.4-mm) LOP test pieces are listed in Tables 7 and 8 and plotted in the S-N diagram of Fig. 12. As with the 3/8-in. (9.6-mm) LOP welds, a large amount of scatter in the data resulted from the variation in

defect width ($2c_o$). The fatigue lives of almost all the LOP test pieces were shorter than those of sound welds: see Fig. 12.

The RR LOF test results for both the 3/8 and 1-in. (9.6 and 25.4-mm) test pieces are given in Tables 9 and 10 and plotted in Figs. 11 and 12. Figures 11 and 12 indicate that the LOF defects produce fatigue lives which are about the same or slightly less than sound RR welds. The RR LOF test pieces gave greater fatigue lives than most LOP specimens. This result is not surprising since the projected widths (ℓ_o) of the LOF defects are generally smaller than of the width of most of the LOP containing test pieces.

4.5 Results for Strain Controlled Fatigue Testing

Results of the completely reversed strain controlled fatigue tests of 5083 base metal and 5183 weld metal are presented in Figs. 13 and 14 and Table 17. The cyclic stress-strain parameters were determined for the 5183 weld metal using the methods of Raske and Morrow (10) these data are also listed in Table 17. A comparison of the fatigue resistance at lives greater than 10^3 reversals shows that the 5183 weld metal can sustain a greater amount of reversed strain than the 5083-0 base metal; however, this difference is not large.

5. DISCUSSION

5.1 Influence of Full Length LOP Defects

As shown in Figs. 11 and 12, full length LOP defects have a profound effect on fatigue life. Defects of large width are substantially more serious than smaller width defects. This tendency is illustrated in Figs. 17-20 in which the relationship between defect width ($2c_o$ or ℓ_o) and fatigue life is shown for each thickness and stress range. The solid lines in these figures are predictions which will be discussed in a subsequent section. Both the reinforcement intact (RI) and reinforcement removed (RR) test pieces gave substantially the same lives. Naturally, the difference between sound RR test pieces and LOP containing RR test pieces is substantially greater than the difference between sound RI welds and these with LOP.

If one uses sound RI welds as a norm, the best fit curves (solid lines of Fig. 12) would indicate that only the very smallest LOP defects tested (~ 0.05-in.) would give lives equal to or greater than the average expectancy for sound RI welds. If one considers that sound RI welds can give lives as small as 3×10^4 cycles at 19 ksi and 2×10^5 cycles at 12 ksi, then from Figs. 18-21, it would seem that LOP defects as large as 0.07 to 0.10-in. in width could be permitted if one could accurately measure their width using conventional NDT techniques. As will be subsequently discussed, this is probably not possible.

5.2 Influence of Intermittent LOF defects

Althouth the shape, inclination and length of the "natural" LOP defects was radically different from the full length LOP defects (see Figs. 6-9),

it was found that the results for these LOF defects were similar to the LOP results when considered on the basis of width projected onto a plane normal to the tensile stress (ℓ_o): see Fig. 4. As seen in Figs. 18-21, an LOF of given projected width (ℓ_o) gives approximately the same result as a similar width LOP.

This finding leads to the following conclusions: the effect of an LOF defect of projected width (ℓ_o) is essentially similar to the effect of a full length LOP of similar width. Furthermore, the finite lengths of the LOF defects had no appreciable influence on their behavior.

5.3 Predictions of Total Fatigue Life, N_T

The total fatigue life of a weld may be considered to be composed of a crack initiation period (N_I) and a crack propagation period (N_p). Strain-controlled, smooth-specimen fatigue data such as that shown in Figs. 13 and 14 and Table 17 can be used to calculate the fatigue crack initiation period using the method of Topper, Morrow, Martin, and Mattos (11,12,13,14). This method considers fatigue crack initiation to have occurred when a hypothetical filament of metal situated at the tip of the notch (LOP in the present circumstance) fails by the accumulation of fatigue damage. This calculation is carried out using a computer simulation of the hysteresis loop of the material at the notch tip, (weld metal in this case). The scheme of the computation is diagrammed in Fig. 15 and the use of the model requires:

1. Determination of the elastic stress concentration factor of the notch (K_t). For an eliptical flaw in a finite plate K_t is (15):

$$K_t = 1 + 2 \left[\frac{c}{r} \sec \frac{\pi c}{w}\right]^{\frac{1}{2}} \qquad (1)$$

2. Estimation of the fatigue notch factor (K_f) from K_t through the use of Peterson's equation (16):

$$K_f = 1 + \frac{K_t - 1}{1 + \frac{a}{r}} \tag{2}$$

3. Knowledge of the cyclic stress-strain properties of the material at the notch root: n', K', etc.

4. Knowledge of the strain-life properties at the notch root: σ_f', ε_f', b, c, etc.

The nominal stresses (S) are related to the notch root stresses and strains through the use of Neuber's Rule which governs the maximum value of the product ($\sigma \cdot \varepsilon$) attained in a given reversal:

$$\sigma \cdot \varepsilon = \frac{(K_f S)^2}{E} \tag{3}$$

Damage is calculated on a reversal by reversal basis by the computer simulation from the relationship:

$$\frac{1}{2N_f} = \left[\left(\frac{1}{2N_f}\right)_e \text{ or } \left(\frac{1}{2N_f}\right)_p \right] + \left(\frac{1}{2N_f}\right)_o \tag{4}$$

where: $\left(\frac{1}{2N_f}\right)_e$ is the damage per reversal resulting from the elastic strain amplitude

$\left(\frac{1}{2N_f}\right)_p$ is the damage per reversal resulting from a plastic strain amplitude

$\left(\frac{1}{2N_f}\right)_o$ is the additional damage resulting from the presence of a mean stress.

For the present calculations, the level of plastic strains were so low that essentially no mean stress relaxation occurred, and the mean stress was therefore considered to be constant. The computer program simulated the cyclic hardening and softening of the material. Failure of the hypothetical filament was considered to occur when:

$$\sum \frac{1}{2N_f} (2N_i) = 1 \qquad (5)$$

Values of K_f were determined using Eqs. 1 and 2. It can be shown that K_f achieves a maximum value ($K_{f\ max}$) for a critical value of (r) which is of the order of (a) in Peterson's Equation. Values of $K_{f\ max}$ were used in this calculation since it is believed to be physically realistic that a radius equal to that giving $K_{f\ max}$ should exist somewhere along the length of the LOP defect. In addition, this assumption gives the most pessimistic estimates of N_I. Values of $K_{f\ max}$ are plotted as a function of plate width and LOP width in Fig. 16.

The results of these calculations are summarized in Fig. 17 in which the relationship between a given severity of LOP (i.e., $K_{f\ max}$) and cylces to crack initiation (N_I) is given. Actual predictions of N_I are plotted in Figs. 18-21.

The fatigue crack propagation portion of life (N_p) was estimated using the power law model for fatigue crack growth (17):

$$\frac{dc}{dN} = C(\Delta K)^n \qquad (6)$$

which can be numerically integrated to give:

$$N_p = \frac{1}{C} \int_{c_o}^{c_f} (\Delta K)^{-n}\, dc \qquad (7)$$

where ΔK for the LOP defect in a finite width plate is taken as (18):

$$\Delta K = \Delta S \left[\pi c \sec \frac{\pi c}{w}\right]^{\frac{1}{2}} \qquad (8)$$

where: N_p = fatigue crack propagation life

ΔK = range in stress intensity

$\frac{dc}{dN}$ = fatigue crack growth rate

C,n = material properties

c_o = initial defect width

c_f = final defect width

The calculated values of N_p are very sensitive to the initial value of defect length (c_o) and to the material properties C and n. The initial defect length (c_o) was taken as the half-width of the LOP at its widest point or at the point where crack propagation originated. In those cases where the measured value of c_o gave ΔK values less than reported values of ΔK_{th} (8 ksi $\sqrt{in.}$), then the c_o defined by ΔK_{th} for the stress range in question was used. The final value of crack length (c_f) was taken as one-half the plate thickness. The material properties, C and n used inthe calculations are listed in Table 17 and are measured values for 5083 base metal under R = 0 conditions (19). The limited information available on the C and n values for weld metal would indicate that weld metal is similar to or slightly more resistant to fatigue crack growth than base metal (20).

Values of N_p calculated using the above method are plotted in Figs. 18-21. The total fatigue life (N_T) was calculated as the sum of N_I and N_p and is also plotted in these figures.

The calculated and measured total lives shown in Figs. 18-21 are in good general agreement. A surprisingly large fraction of life is devoted to crack initiation. The initiation and propagation lives become equal in the life region of 10^4 and 10^5 cycles. At greater lives, crack initiation appears to dominate. At the lower stress level (12 ksi) and particularly for the 3/8-in. specimens, crack initiation appears to play a predominant role. At the higher stress levels and particularly for the 1-in. specimens, propagation dominates.

5.4 Effectiveness of NDT Evaluation

As argued in Sections 5.1 and 5.2, all but the smallest width LOP and LOF defects must be considered rejectable. As seen in Tables 11-16, all LOP and LOF specimens were rejected by the current U.S. Navy radiographic standards which are reproduced in Appendix B. Although these standards are based on the length rather than the through-thickness width of the defect which latter dimension was shown to control, the effect of these current standards was to disallow any of the LOP and LOF defects, albeit, for the wrong reason.

In contrast to the radiographic standards, the ultrasonic inspection standards, reproduced in Appendix A, are based both upon defect length and width by reason of the fact that defects giving indications below a disregard level are to be ignored regardless of their apparent length.

Each specimen was examined using the current Navy ultrasonic test code (4) and calibration block. As seen in Figs. 22 and 23, very few of the LOP and LOF specimens were rejectable, and there is no apparent pattern to those which fall into the Class II and III categories. In the light of the above

observations, it must be concluded that the current USN ultrasonic test standards are rather unconservative as regards the defects studied here.

In summary, neither normal incidence radiography or conventional ultrasonic test methods can reliably measure the controlling through-the-thickness dimension of the LOP type defect with the precision necessary to discriminate between serious and ignorable defects. Since LOP and LOF defects larger than about 0.1-in. in width were shown to drastically reduce the fatigue life by amounts generally larger than a factor of ten, it would seem that any LOP or LOF indication should be rejected to insure fatigue lives no less than that of sound RI welds. The current ultrasonic code would seem to be quite unconservative. The current radiographic code, although based upon a dimension having little influence, has the effect of rejecting serious LOP and LOF defects and would therefore seem justified.

6. CONCLUSIONS

1. Lack of penetration (LOP) defects can seriously reduce the fatigue life of both reinforcement intact and reinforcement removed welds. The magnitude of this reduction is determined by the through-thickness dimension of the LOP. The porosity associated with these defects seemed to exert no influence.
2. Less than full length, inclined lack-of-fusion (LOF) defects were generally less serious than LOP defects but if compared with LOP defects on the basis of width projected normal to the tensile stress, they were found to follow the same trends as equivalent width LOP. The length of the LOF along the axis of the weld seemed to have no influence on their effect.
3. Predictions of total fatigue life (N_T) based upon separate, conservative estimates of the crack initiation period (N_I) and crack propagation life (N_P) agreed well with the experimental data. A surprisingly large reaction of life was attributable to crack initiation.
4. The current ultrasonic NDT standards did not discriminate between acceptable and unacceptable LOP or LOF defects, and this standard seems quite unconservative. The current radiographic standard seems stringent enough in that all LOP and LOF defects were rejected, and this rejection would seem warranted by the test results. Neither NDT standard is rational in the sense that it is not based upon the controlling defect dimension, the through thickness width.

7. REFERENCES

1. Lawrence, F. V. Jr. and Munse, W. H., "Effects of Porosity on the Tensile Properties of 5083 and 6061 Aluminum Alloy Weldments," WRC Bull. 181, New York, 1973.

2. Lawrence, F. V. Jr., Munse, W. H. and Burk, J. D., "Effects of Porosity on the Fatigue Properties of 5083 Aluminum Alloy Weldments," WRC Bull. 206, New York, 1975.

3. Dinsdale, W. O. and Young, J. G., "Significance of Defects in Aluminum Alloy Fusion Welds," Weld. Res., 9, 8, 1962.

4. *Ultrasonic Inspection Procedure and Acceptance Standards for Hull Structure Production and Repair Welds*, NAVSHIPS 0900-006-3010, Naval Sea Systems Command, January 1966.

5. *Radiographic Standards for Production and Repair Welds*, NAVSHIPS 0900-003-9000, Naval Sea Systems Command, March 1967.

6. Sanders, W. W. and Gannon, S. M., "Fatigue Behavior of Aluminum Alloy 5083 Butt Welds," WRC Bull. 199, New York, 1974.

7. Feltner, C. E. and Mitchell, M. R., "Basic Research on the Cyclic Deformation and Fracture Behavior of Materials," Manual on Low Cycle Fatigue Testing, ASTM STP 465, 27, 1969.

8. Martin, J. F., "Cyclic Stress-Strain Behavior and Fatigue Resistance of Two Structural Steels," University of Illinois FCP Report No. 9, 1973.

9. Burk, J. D. and Lawrence, F. V. Jr., "Influence of Bending Stresses on the Fatigue Crack Propagation Life in Butt Welds," Submitted to Welding Journal for publication, March 1976.

10. Raske, D. T. and Morrow, JoDean, "Mechanics of Materials in Low Cycle Fatigue Testing," Manual of Low Cycle Fatigue Testing, ASTM STP 465, 1969.

11. Topper, T. H. and Morrow, JoDean, "Simulation of the Fatigue Behavior at the Notch Root in Spectrum Loaded Notched Members," University of Illinois TAM Report No. 333, 1970.

12. Morrow, JoDean, "Fatigue Properties of Metals, Fatigue Design Handbook, SAE, 4, 3.2, 1968.

13. Martin, J. F., "Fatigue Damage Analysis for Irregular Shaped Structures Subjected to Representative Loads," University of Illinois FCP Report No. 10, 1973.

14. Mattos, R. J., "Estimation of the Fatigue Crack Initiation Life in Welds Using Low Cycle Fatigue Concepts," University of Illinois, Ph.D. Thesis, 1975.

15. Peterson, R. E., Stress Concentration Factors, Wiley & Sons, New York, 1974.

16. Peterson, R. E., Metal Fatigue, Chapter 13, Sines and Waisman (ed.), McGraw-Hill, 1959.

17. Paris, P. C. and Erdogan, F., "A Critical Analysis of Crack Propagation Laws," J. Basic Eng. ASME Trans. Series D, 85, 528, 1963.

18. Tada, H., Paris, P. D. and Irwin, G. R., The Stress Analysis of Cracks Handbook, Del Research Corp., Hellertown, PA., 1973.

19. Nordmark, G. E., Private Communication, Alcoa Technical Center, Alcoa Center, PA., 1976.

20. Kaufman, J. G. and Kelsey, R. A., "Fracture Toughness and Fatigue Properties of 5083-O Plate and 5183 Welds for Liquified Natural Gas Applications," ASTM STP 579,138, 1975.

TABLE 1 Monotonic Tension
Properties of 5083-O Aluminum and 5183
Aluminum Weld Metal

Material Property	5083	5183
Modulus of Elasticity, ksi (MPa)	10,300 (71,015)	10,300 (71,015)
Yield Strength (0.2% offset), ksi (MPa)	19.0 (131.0)	20.5 (141.3)
Ultimate Strength, ksi (MPa)	43.5 (300.0)	44.2 (304.7)
True Fracture Strength, ksi (MPa)	61.2 (421.8)	62.4 (430.0)
True Fracture Ductility	0.36	0.40

TABEL 2 Typical Chemical Composition
of Base and Filler Metals

Aluminum	Composition in wieght percent								
	Si	Fe	Cu	Mn	Mg	Cr	Zn	Ti	Al
5083 (BM)	0.14	0.22	0.05	0.64	4.50	0.08	0.04	0.03	Bal.
5183 (FM)	0.12	0.17	0.02	0.57	4.96	0.07	0.03	0.09	Bal.

TABLE 3 Specimen Notation

Program Test Group	Defect Severity Level (only for LOP welds)	Plate Machined From	Specimen Number
P 1	4	2	5

Program Test Group: P1 - Reinforcement intact (RI) as-welded LOP welds

P2 - Reinforcement removed (RR) LOP welds

P3 - Reinforcement removed (RR) LOF welds

Defect Severity Level: 1 - sound

2 - small

3 - medium

4 - large

Plate Machined From: 1,2,3, ect. (to specify a welded panel)

Specimen Number: 1,2,3,4,5, etc. (to distinguish between specimens in a test series)

TABLE 4 Test Results 3/8-in. Reinforcement Intact LOP Welds

Specimen	ΔS, ksi (MPa) R=0	$2c_o$, in. (mm)	w, in. (mm)	N_f cycles
Small				
P1-2-3-1	19 (131.0)	toe failure	0.38 (9.6)	2,233
P1-2-2-2	19 (131.0)	0.06 (1.52)	0.45 (11.4)	15,060
P1-2-2-3	19 (131.0)	0.06 (1.52)	0.52 (13.2)	31,690
P1-2-2-4	12 (82.7)	0.02 (0.51)	0.54 (13.7)	1,927,120
P1-2-2-5	12 (82.7)	0.06 (1.52)	0.52 (13.2)	413,920
P1-2-2-6	12 (82.7)	0.05 (1.27)	0.52 (13.2)	2,012,000
Medium				
P1-3-1-1	19 (131.0)	0.10 (2.54)	0.50 (12.7)	14,940
P1-3-1-2	19 (131.0)	0.08 (2.03)	0.52 (13.2)	14,050
P1-3-1-3	19 (131.0)	0.07 (1.78)	0.52 (13.2)	10,405
P1-3-1-4	12 (82.7)	0.08 (2.03)	0.52 (13.2)	546,190
P1-3-1-5	12 (82.7)	0.07 (1.78)	0.50 (12.7)	189,370
P1-3-1-6	12 (82.7)	0.07 (1.78)	0.50 (12.7)	564,500
Large				
P1-4-1-1	19 (131.0)	0.12 (3.05)	0.50 (12.7)	5,980
P1-4-1-2	19 (131.0)	0.16 (4.06)	0.47 (11.9)	7,620
P1-4-1-3	19 (131.0)	0.10 (2.54)	0.48 (12.2)	5,975
P1-4-1-4	12 (82.7)	0.11 (2.79)	0.54 (13.7)	74,570
P1-4-1-5	12 (82.7)	0.18 (4.57)	0.50 (12.7)	54,630
P1-4-3-6	12 (82.7)	0.08 (2.03)	0.52 (13.2)	133,880

TABLE 5 Test Results 3/8-in. Reinforcement Removed LOP Welds

Specimen	ΔS, ksi (MPa) R=0	$2c_o$, in. (mm)	w, in. (mm)	N_f cycles
Small				
P2-2-1-1	12 (82.7)	0.02 (0.51)	0.38 (9.6)	1,356,690
P2-2-1-2	19 (131.0)	0.10 (2.54)	0.38 (9.6)	13,770
P2-2-1-3	12 (82.7)	0.04 (1.02)	0.38 (9.6)	245,050
P2-2-1-4	12 (82.7)	0.08 (2.03)	0.38 (9.6)	326,202
P2-2-1-5	19 (131.0)	0.08 (2.03)	0.38 (9.6)	40,340
P2-2-1-6	19 (131.0)	0.13 (3.30)	0.38 (9.6)	45,490
Medium				
P2-3-2-1	19 (131.0)	0.14 (3.56)	0.38 (9.6)	6,790
P2-3-2-2	19 (131.0)	0.16 (4.06)	0.38 (9.6)	5,030
P2-3-2-3	19 (131.0)	0.13 (3.30)	0.38 (9.6)	6,150
P2-3-2-5	12 (82.7)	0.06 (1.52)	0.38 (9.6)	398,700
P2-3-2-6	12 (82.7)	0.14 (3.56)	0.38 (9.6)	61,940
P2-3-3-7	12 (82.7)	0.15 (3.81)	0.38 (9.6)	12,960
Large				
P2-4-2-1	19 (131.0)	0.21 (5.33)	0.38 (9.6)	1,411
P2-4-2-2	19 (131.0)	0.14 (3.56)	0.38 (9.6)	1,535
P2-4-2-3	19 (131.0)	0.18 (4.57)	0.38 (9.6)	1,742
P2-4-2-4	12 (131.0)	0.16 (4.06)	0.38 (9.6)	9,210
P2-4-2-5	12 (131.0)	0.15 (3.81)	0.38 (9.6)	5,700
P2-4-3-6	12 (131.0)	0.10 (2.54)	0.38 (9.6)	632,500

TABLE 6 Test Results 1-in. Reinforcement Intact LOP Welds

Specimen	ΔS, ksi (MPa) R=0	$2c_o$, in. (mm)	w, in. (mm)	N_f cycles
Small				
P1-2-1-1	19 (131.0)	0.12 (3.05)	1.08 (27.4)	16,850
P1-2-1-2	19 (131.0)	0.10 (2.54)	1.08 (27.4)	10,940
P1-2-1-3	19 (131.0)	0.10 (2.54)	1.08 (27.4	13,840
P1-2-1-4	12 (82.7)	toe failure	1.08 (27.4)	506,250
P1-2-2-5	12 (82.7)	0.17 (4.32)	1.08 (27.4)	292,670
P1-2-3-6	12 (82.7)	0.18 (4.57)	1.08 (27.4)	229,610
Medium				
P1-3-1-1	19 (131.0)	0.18 (4.57)	1.08 (27.4)	4,070
P1-3-1-2	19 (131.0)	0.24 (6.10)	1.08 (27.4)	3,830
P1-3-1-3	19 (131.0)	0.20 (5.08)	1.08 (27.4)	3,210
P1-3-1-4	12 (82.7)	0.25 (6.35)	1.08 (27.4)	31,990
P1-3-2-5	12 (82.7)	0.12 (3.05)	1.08 (27.4)	135,870
P1-3-2-6	12 (82.7)	0.20 (5.08)	1.08 (27.4)	248,530
Large				
P1-4-1-1	19 (131.0)	0.24 (6.10)	1.08 (27.4)	6,040
P1-4-1-2	19 (131.0)	0.20 (5.08)	1.08 (27.4)	3,920
P1-4-1-3	19 (131.0)	0.18 (4.57)	1.08 (27.4)	4,560
P1-4-1-4	12 (82.7)	0.19 (4.83)	1.08 (27.4)	107,000
P1-4-2-5	12 (82.7)	0.22 (5.59)	1.08 (27.4)	59,900
P1-4-2-6	12 (82.7)	0.24 (6.10)	1.08 (27.4)	114,600

TABLE 7 Test Results 1-in. Reinforcement Removed LOP Welds

Specimen	ΔS, ksi (MPa) R=0	$2c_o$, in. (mm)	w, in. (mm)	N_f cycles
Small				
P2-2-2-1	12 (82.7)	0.06 (1.52)	1.00 (25.4)	326,000
P2-2-2-2	19 (131.0)	0.16 (4.06)	1.00 (25.4)	37,640
P2-2-2-3	19 (131.0)	0.10 (2.54)	1.00 (25.4)	17,640
P2-2-3-4	12 (82.7)	0.04 (0.76)	1.00 (25.4)	196,900
P2-2-3-5	12 (82.7)	0.04 (1.02)	1.00 (25.4)	110,700
P2-2-3-6	12 (82.7)	0.02 (0.51)	1.00 (25.4)	424,500
Medium				
P2-3-2-1	19 (131.0)	0.10 (2.54)	1.00 (25.4)	7,320
P2-3-2-2	19 (131.0)	0.15 (3.81)	1.00 (25.4)	8,720
P2-3-2-3	19 (131.0)	0.18 (4.06)	1.00 (25.4)	7,940
P2-3-3-4	12 (82.7)	0.18 (4.57)	1.00 (25.4)	149,400
P2-3-3-5	12 (82.7)	0.15 (3.81)	1.00 (25.4)	190,400
P2-3-3-6	12 (82.7)	0.12 (3.05)	1.00 (25.4)	225,400
Large				
P2-4-2-1	12 (82.7)	0.21 (5.33)	1.00 (25.4)	40,760
P2-4-2-2	19 (131.0)	0.22 (5.59)	1.00 (25.4)	3,170
P2-4-2-3	19 (131.0)	0.24 (6.10)	1.00 (25.4)	3,240
P2-4-3-4	12 (82.7)	0.30 (7.62)	1.00 (25.4)	17,870
P2-4-3-5	12 (82.7)	0.32 (8.13)	1.00 (25.4)	16,330
P2-4-3-6	12 (82.7)	0.30 (7.62)	1.00 (25.4)	40,850

TABLE 8 Test Results 3/8 in. Reinforcement Removed LOF Welds

Specimen	ΔS, ksi (MPa) R-0	ℓ, in. (mm)	ℓ_o, in. (mm)	w, in. (mm)	s, in. (mm)	β, degrees (radians)	N_f cycles
P3-1-1	19 (131.0)	0.28 (7.11)	0.08 (2.03)	0.38 (9.65)	0.14 (3.56)	90 (1.57)	46,070
P3-1-2	19 (131.0)	0.24 (6.10)	0.07 (1.78)	0.38 (9.65)	0.12 (3.05)	90 (1.57)	34,970
P3-1-3	12 (82.7)	0.30 (7.62)	0.08 (2.03)	0.38 (9.65)	0.10 (2.54)	90 (1.57)	887,280
P3-1-4	12 (82.7)	0.29 (7.37)	0.08 (2.03)	0.38 (9.65)	0.11 (2.79)	90 (1.57)	886,910
P3-1-5	12 (82.7)	0.25 (6.35)	0.06 (1.52)	0.38 (9.65)	0.11 (2.79)	90 (1.57)	2,538,330
P3-2-6	19 (131.0)	0.22 (5.59)	0.05 (1.27)	0.38 (9.65)	0.15 (3.81)	90 (1.57)	48,730
P3-2-7	19 (131.0)	0.27 (6.86)	0.05 (1.27)	0.38 (9.65)	0.14 (3.56)	90 (1.57)	348, 120
P3-2-8	19 (131.0)	0.22 (5.59)	0.05 (1.27)	0.38 (9.65)	0.14 (3.56)	90 (1.57)	259,940
P3-2-9	12 (82.7)	0.23 (5.85)	0.07 (1.78)	0.38 (9.65)	0.15 (3.81)	90 (1.57)	1,719,770
P3-2-10	12 (82.7)	0.26 (6.60)	0.08 (2.03)	0.38 (9.65)	0.14 (3.56)	90 (1.57)	1,040,590
P3-3-11	19 (131.0)	0.19 (4.83)	0.06 (1.57)	0.38 (9.65)	0.13 (3.30)	90 (1.57)	737,370
P3-3-12	12 (82.7)	0.20 (5.08)	0.05 (1.27)	0.38 (9.65)	0.16 (4.06)	90 (1.57)	10,000,000+

TABLE 9 Test Results 1-in. Reinforcement Removed LOF Welds

Specimen	ΔS, ksi (MPa) R=0	ℓ, in. (mm)	ℓ_o, in. (mm)	w, in. (mm)	s, in. (mm)	β, degrees (radians)	N_f cycles
P3-2-2	19 (131.0)	0.64 (16.2)	0.12 (3.05)	1.06 (26.9)	0.25 (6.35)	90 (1.57)	45,000
P3-2-3	12 (82.7)	0.40 (10.2)	0.11 (2.79)	1.06 (26.9)	0.38 (.65)	90 (1.57)	1,989,000
P3-2-5	12 (82.7)	0.56 (11.7)	0.18 (4.57)	1.06 (26.9)	0.42 (10.7)	90 (1.57)	5,038,000+
P3-3-6	12 (82.7)	0.68 (17.3)	0.30 (7.62)	1.06 (26.9)	0.36 (9.14)	90 (1.57)	1,222,010
P3-3-7	12 (82.7)	0.60 (10.2)	0.12 (3.05)	1.06 (26.9)	0.34 (8.64)	90 (1.57)	222,830
P3-3-8	12 (82.7)	0.62 (15.7)	0.10 (2.54)	1.06 (26.9)	0.40 (10.2)	90 (1.57)	407,180
P3-3-9	19 (131.0)	0.54 (13.7)	0.15 (3.81)	1.06 (26.9)	0.36 (9.14)	90 (1.57)	59,140
P3-3-10	19 (131.0)	0.58 (14.7)	0.20 (5.08)	1.06 (26.9)	0.30 (7.62)	90 (1.57)	9,810
P3-4-13	12 (82.7)	0.10 (2.54)	0.08 (2.03)	1.06 (26.9)	0.36 (9.14)	90 (1.57)	400,620
P3-4-14	12 (82.7)	0.20 (.08)	0.10 (2.54)	1.06 (26.9)	0.40 (10.2)	90 (1.57)	456,620

TABLE 10 Test Results for Sound Welds

Specimen	ΔS, ksi (MPa) R=0	N_f cycles	Radiographic Class	Ultrasonic NDT Class	Plate thickness t, in. (mm)
P1-1-1-1	19 (131.0)	21,040	I	I	3/8 (9.6)
P1-1-1-2	19 (131.0)	27,720	I	I	3/8 (9.6)
P1-1-1-3	19 (131.0)	29,400	I	I	3/8 (9.6)
P1-1-1-4	12 (82.7)	135,680	I	I	3/8 (9.6)
P1-1-1-5	12 (82.7)	205,350	I	I	3/8 (9.6)
P1-1-1-6	12 (82.7)	153,080	I	I	3/8 (9.6)
P1-1-5-7	12 (82.7)	514,800	I	I	3/8 (9.6)
P1-1-5-9	12 (82.7)	213,510	I	I	3/8 (9.6)
P1-1-5-10	19 (131.0)	46,950	I	I	3/8 (9.6)
P1-1-5-11	19 (131.0)	61,480	I	I	3/8 (9.6)
P1-1-5-12	19 (131.0)	22,580	I	I	3/8 (9.6)
P1-1-1-1	19 (131.0)	96,900	I	I	1 (25.4)
P1-1-1-2	19 (131.0)	114,790	I	I	1 (25.4)
P1-1-1-3	19 (131.0)	132,600	I	I	1 (25.4)
P1-1-1-4	12 (82.7)	1,224,530	I	I	1 (25.4)
P1-1-1-5	12 (82.7)	1,163,050	I	I	1 (25.4)
P1-1-1-6	12 (82.7)	2,135,600	I	I	1 (25.4)

TABLE 11 3/8-in. RI LOP

Specimen	ΔS, ksi (MPa) R=0	N_f cycles	Radiographic Class	Ultrasonic NDT Class	Fracture Surface Appearance
P1-2-3-1	19 (131.0)	2,233	Reject	I	Weld toe failure
P1-2-2-2	19 (131.0)	15,060	Reject	I	Large pore associated with LOP
P1-2-2-3	19 (131.0)	31,690	Reject	I	No porosity associated with LOP
P1-2-2-4	12 (82.7)	1,927,120	Reject	I	Large pores associated with LOP
P1-2-2-5	12 (82.7)	413,920	Reject	I	Large pores associated with LOP
P1-2-2-6	12 (82.7)	2,012,000	Reject	I	Small porosity associated with LOP
P1-3-1-1	19 (131.0)	14,940	Reject	II,III	No porosity associated with LOP
P1-3-1-2	19 (131.0)	14,050	Reject	I	No porosity associated with LOP
P1-3-1-3	19 (131.0)	10,405	Reject	I	Small porosity associated with LOP
P1-3-1-4	12 (82.7)	546,190	Reject	I	Small porosity associated with LOP
P1-3-1-5	12 (82.7)	189,370	Reject	I	Small porosity associated with LOP
P1-3-1-6	12 (82.7)	564,500	Reject	I	No porosity associated with LOP
P1-4-1-1	19 (131.0)	5,980	Reject	I	Small porosity associated with LOP
P1-4-1-2	19 (131.0)	7,620	Reject	I	Large porosity associated with LOP
P1-4-1-3	19 (131.0)	5,975	Reject	I	Extremely large porosity associated with LOP
P1-4-1-4	12 (82.7)	74,570	Reject	II,III	Extremely large porosity associated with LOP
P1-4-1-5	12 (82.7)	59,630	Reject	I	Extremely large porosity associated with LOP
P1-4-1-6	12 (82.7)	133,880	Reject	I	Extremely large porosity associated with LOP

TABLE 12 3/8-in. RR LOP

Specimen	ΔS, ksi (MPa) R=0	N_f cycles	Radiographic Class	Ultrasonic NDT Class	Fracture Surface Appearance
P2-2-1-1	12 (82.7)	1,356,690	Reject	I	Intermittent LOP
P2-2-1-2	19 (131.0)	13,770	Reject	I	Large porosity associated with LOP
P2-2-1-3	12 (82.7)	245,050	Reject	I	Large porosity associated with LOP
P2-2-1-4	19 (131.0)	326,020	Reject	I	Large porosity associated with LOP
P2-2-1-5	19 (131.0)	40,340	Reject	I	Large porosity associated with LOP
P2-2-1-6	19 (131.0)	45,490	Reject	I	Large porosity associated with LOP
P2-3-2-1	19 (131.0)	6,790	Reject	I	Small porosity associated with LOP
P2-3-2-2	19 (131.0)	6,150	Reject	I	Small porosity associated with LOP
P2-3-2-3	19 (131.0)	6,150	Reject	I	Small porosity associated with LOP
P2-3-2-5	12 (82.7)	298,700	Reject	I	Small porosity associated with LOP
P2-3-2-6	12 (82.7)	61,940	Reject	I	Small porosity associated with LOP
P2-3-3-7	12 (82.7)	12,960	Reject	I	Large porosity associated with LOP
P2-4-2-1	19 (131.0)	1,411	Reject	II,III	LOF and porosity associated with LOP
P2-4-2-2	19 (131.0)	1,535	Reject	II,III	LOF and porosity associated with LOP
P2-4-2-3	19 (131.0)	1,742	Reject	I	LOF and porosity associated with LOP
P2-4-2-4	12 (82.7)	9,210	Reject	II,III	Small porosity associated with LOP
P2-4-2-5	12 (82.7)	5,700	Reject	II,III	Small porosity associated with LOP
P2-4-2-6	12 (82.7)	632,560	Reject	I	Worm hole porosity associated with LOP

TABLE 13 1-in. RI LOP

Specimen	ΔS, ksi (MPa) R=0	N_f cycles	Radiographic Class	Ultrasonic NDT Class	Fracture Surface Appearance
P1-2-1-1	19 (131.0)	16,850	Reject	I	Worm hole porosity associated with LOP
P1-2-1-2	19 (131.0)	10,940	Reject	I	Worm hole porosity associated with LOP
P1-2-1-3	19 (131.0)	13,840	Reject	I	Small porosity associated with LOP
P1-2-1-4	12 (82.7)	506,250	Reject	I	Weld toe failure
P1-2-2-5	12 (82.7)	292,670	Reject	I	Worm hole porosity associated with LOP
P1-2-2-6	12 (82.7)	229,610	Reject	I	Worm hole porosity associated with LOP
P1-3-1-1	19 (131.0)	4,070	Reject	I	Small porosity associated with LOP
P1-3-1-2	19 (131.0)	3,830	Reject	II,III	No porosity associated with LOP
P1-3-1-3	19 (131.0)	3,210	Reject	II,III	Worm hole porosity associated with LOP
P1-3-1-4	12 (82.7)	31,990	Reject	II,III	Large porosity associated with LOP
P1-3-2-5	12 (82.7)	135,870	Reject	II,III	Small porosity associated with LOP
P1-3-2-6	12 (82.7)	245,530	Reject	II,III	Small porosity associated with LOP
P1-4-1-1	19 (131.0)	6,040	Reject	I	Small porosity associated with LOP
P1-4-1-2	19 (131.0)	3,920	Reject	I	Medium porosity associated with LOP
P1-4-1-3	19 (131.0)	4,560	Reject	I	Small porosity associated with LOP
P1-4-1-4	12 (82.7)	107,000	Reject	I	No porosity associated with LOP
P1-4-2-5	12 (82.7)	59,900	Reject	I	No porosity associated with LOP
P1-4-2-6	12 (82.7)	114,600	Reject	I	No porosity associated with LOP

TABLE 14 1-in. RR LOP

Specimen	ΔS, ksi (MPa) R=0	N_f cycles	Radiographic Class	Ultrasonic NDT Class	Fracture Surface Appearance
P2-2-2-1	12 (82.7)	326,000	Reject	I	Large porosity associated with LOP
P2-2-2-2	19 (131.0)	37,640	Reject	I	Large porosity associated with LOP
P2-2-2-3	19 (131.0)	17,640	Reject	I	Large porosity associated with LOP
P2-2-3-4	12 (82.7)	196,900	Reject	I	Small porosity associated with LOP
P2-2-3-5	12 (82.7)	110,700	Reject	II,III	No porosity associated with LOP
P2-2-3-6	12 (82.7)	424,500	Reject	I	LOF failure associated with intermitten LOP
P2-3-2-1	19 (131.0)	7,320	Reject	I	Medium porosity associated with LOP
P2-3-2-2	19 (131.0)	8,720	Reject	I	Small porosity associated with LOP
P2-3-2-3	19 (131.0)	7,940	Reject	I	Small porosity associated with LOP
P2-3-3-4	12 (82.7)	149,400	Reject	I	Small porosity associated with LOP
P2-3-3-5	12 (82.7)	190,400	Reject	I	Small porosity associated with LOP
P2-3-3-6	12 (82.7)	225,400	Reject	I	Small porosity associated with LOP
P2-4-2-1	12 (82.7)	40,760	Reject	I	Small porosity associated with LOP
P2-4-2-2	12 (131.0)	3,170	Reject	I	Small porosity associated with LOP
P2-4-2-3	19 (131.0)	3,240	Reject	I	Small porosity associated with LOP
P2-4-3-4	12 (82.7)	17,870	Reject	I	Small porosity associated with LOP
P2-4-3-5	12 (82.7)	16,330	Reject	I	Small porosity associated with LOP
P2-4-3-6	12 (82.7)	40,850	Reject	I	LOF and porosity associated with LOP

TABLE 15 3/8-in. RR LOF

Specimen	ΔS, ksi (MPa) R=0	N_f cycles	Radiographic Class	Ultrasonic NDT Class	Fracture Surface Appearance
P3-1-1	19 (131.0)	46,070	Reject	II,III	Cresent shaped defect
P3-1-2	19 (131.0)	34,970	Reject	I	Cresent shaped defect
P3-1-3	12 (82.7)	887,280	Reject	II,III	Cresent shaped defect
P3-1-4	12 (131.0)	886,910	Reject	II,III	Cresent shaped defect
P3-1-5	12 (82.7)	2,538,330	Reject	II,III	Cresent shaped defect
P3-2-6	19 (131.0)	48,730	Reject	I	Cresent shaped defect
P3-2-7	19 (131.0)	238,120	Reject	I	Cresent shaped defect
P3-2-8	19 (131.0)	259,940	Reject	II,III	Cresent shaped defect
P3-2-9	12 (82.7)	1,719,770	Reject	II,III	Cresent shaped defect
P3-2-10	12 (82.7)	1,040,570	Reject	II,III	Cresent shaped defect
P3-3-11	19 (131.0)	737,370	Reject	I	Cresent shaped defect
P3-3-12	12 (82.7)	10,000,000	Reject	II,III	Cresent shaped defect but did not fail

TABLE 16 1-in. RR LOF

Specimen	ΔS, ksi (MPa) R=0	N_f cycles	Radiographic Class	Ultrasonic NDT Class	Fracture Surface Appearance
P3-2-2	19 (131.0)	45,930	Reject	II,III	Cresent shaped defect
P3-2-3	12 (82.7)	1,989,000	Reject	II,III	Cresent shaped defect
P3-2-4	19 (131.0)	124,320	Reject	I	Cresent shaped defect
P3-2-5	12 (82.7)	5,038,000+	Reject	I	Cresent shaped defect failure in grips
P3-3-6	12 (82.7)	1,222,010	Reject	Reject	Cresent shaped defect failure in grips
P3-3-7	12 (82.7)	222,830	Reject	Reject	Cresent shaped defect failure in grips
P3-3-8	12 (82.7)	407,180	Reject	Reject	Cresent shaped defect failure in grips
P3-3-9	19 (131.0)	59,140	Reject	Reject	Cresent shaped defect failure in grips
P3-3-10	19 (131.0)	9,810	Reject	Reject	Cresent shaped defect failure in grips
P3-4-13	12 (82.7)	400,460	Reject	II,III	Circular blob type defect
P3-4-14	12 (82.7)	456,620	Reject	II,III	Circular blob type defect

TABLE 17

Fatigue Properties of 5083-O Aluminum
and 5183 Aluminum Weld Metal

Property	5183	5083-O
Fatigue Strength Coefficient, σ_f', ksi (MPa)	92.48 (637.2)	105.5 (726.6)
Fatigue Ductility Coefficient, ε_f'	0.581	0.405
Fatigue Strength Exponent, b	-0.107	-0.122
Fatigue Ductility Exponent, c	-0.890	-0.692
Transition Fatigue Life, $2N_f$, reversals	205	845
Cyclic Strength Coefficient, K', ksi (MPa)	73.5 (506.4)	———
Cyclic Strain Harding Exponent, n'	0.0719	———
Cyclic Yield Strength (0.2% offset), ksi (MPa)	39.8 (274.2)	———
Paris Fatigue Crack Growth Rate Coefficient, C, in/cycle (mm/cycle) R=0	———	2×10^{-8} (5.08×10^{-6})
Paris Fatigue Crack Growth Rate Exponent, m, R=0	———	2.7

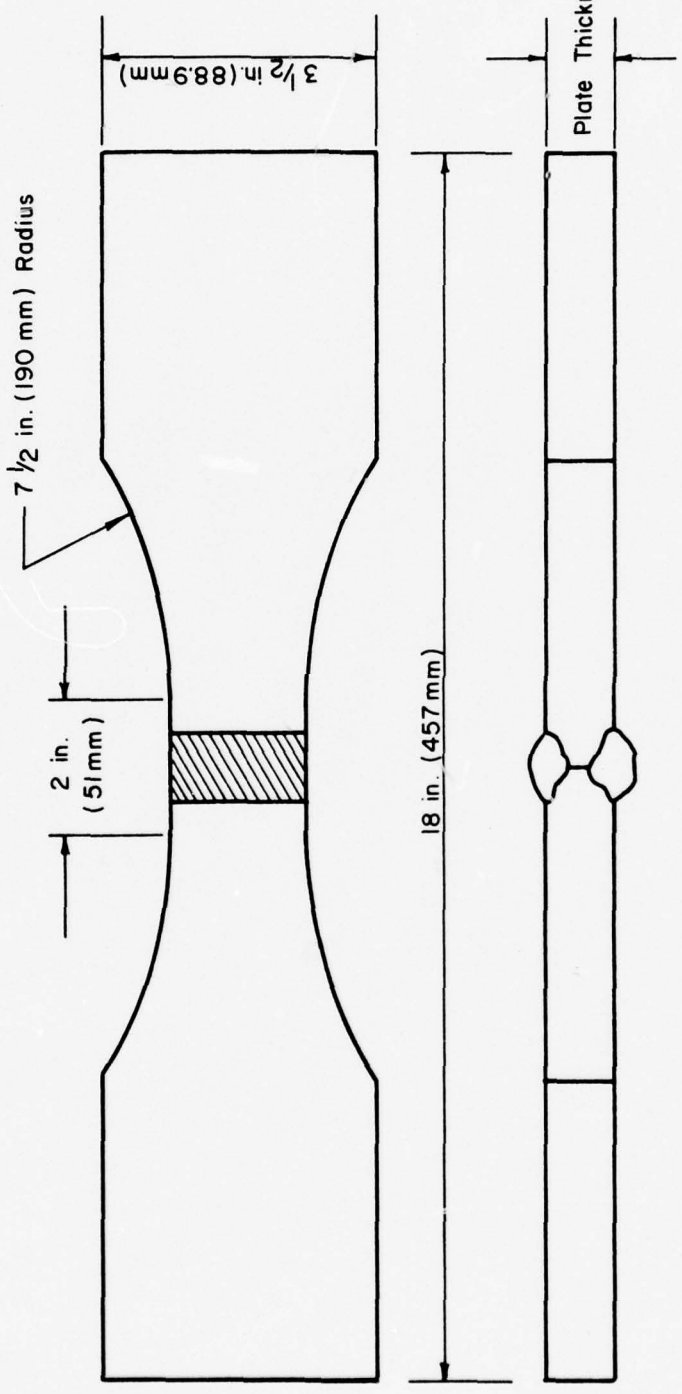

Fig. 1 Geometry for 2-in. (51-mm) wide LOP, 1-in. (25-mm) wide LOP, and 2 1/2-in. (64-mm) wide LOF test pieces

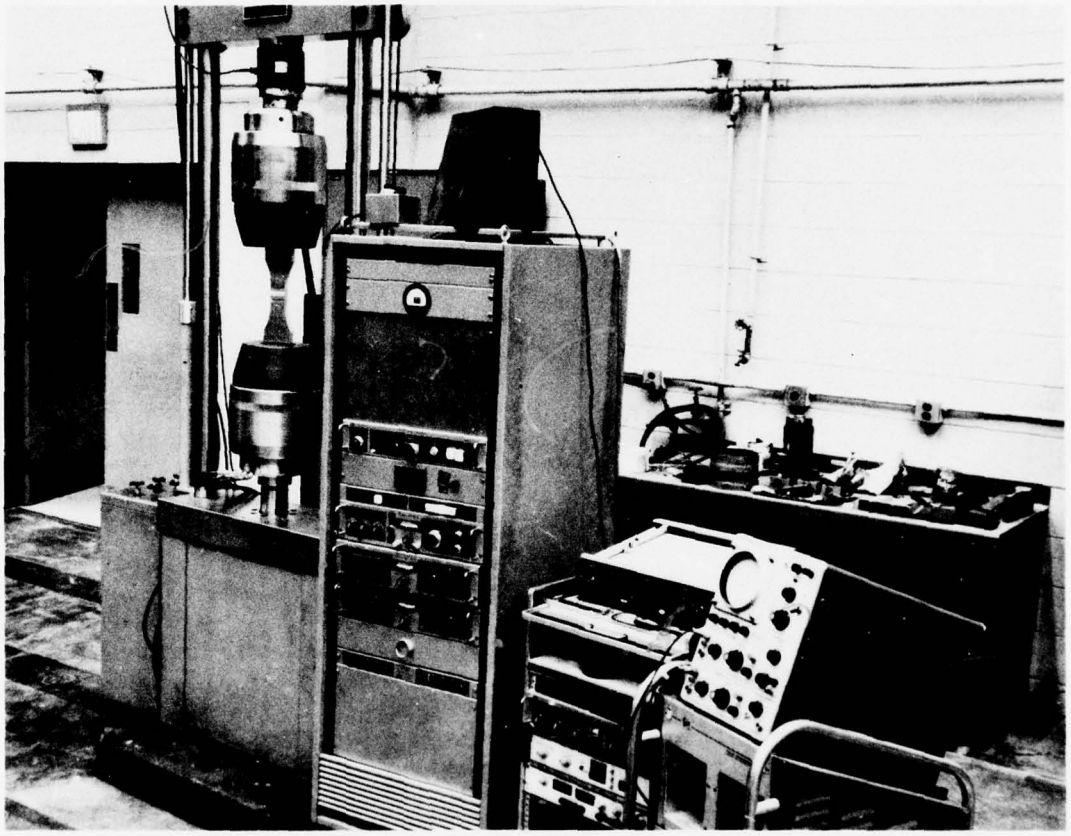

Fig. 2 Fatigue testing apparatus

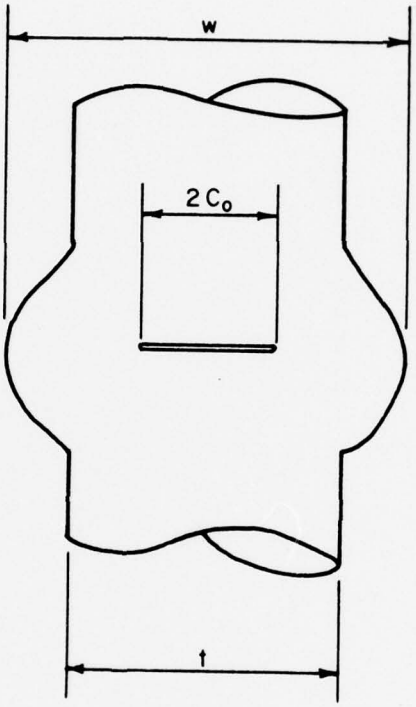

Fig. 3 Width (w), plate thickness (t), and defect width ($2c_o$) describing LOP test piece defects

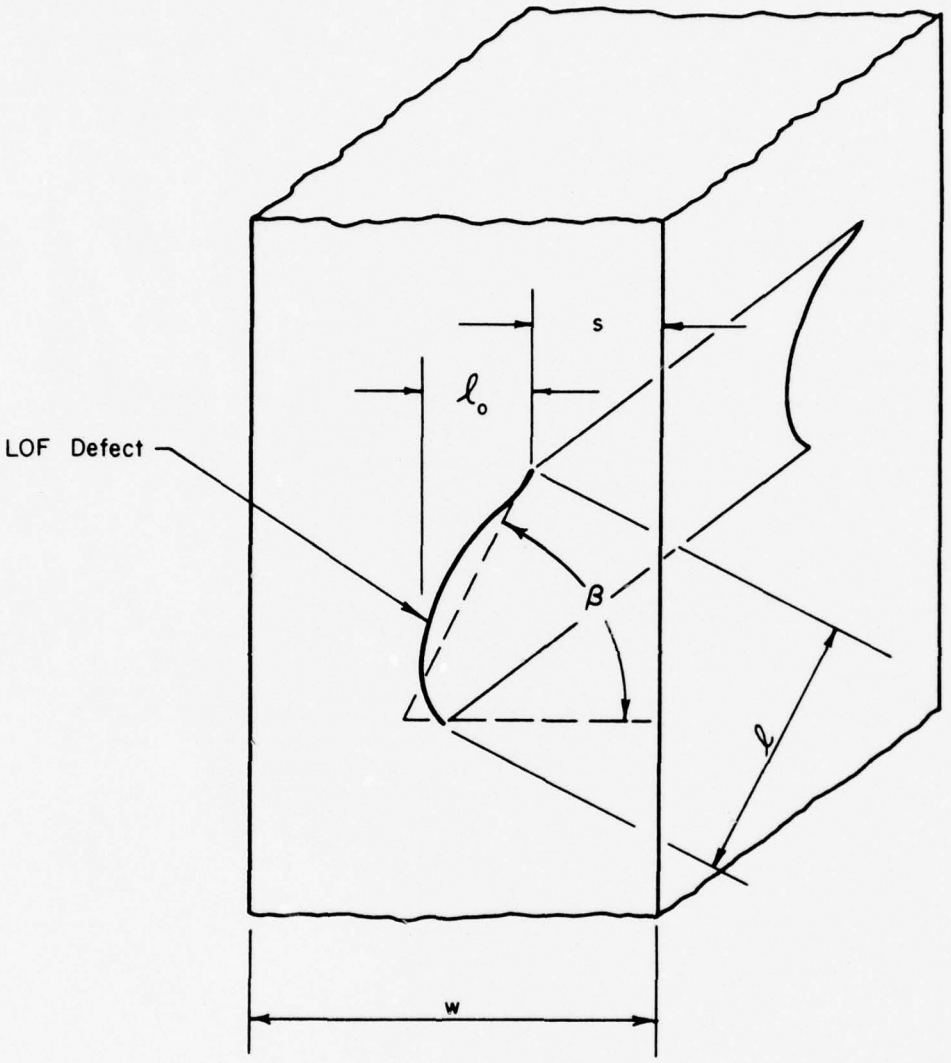

Fig. 4 Width (w), length (ℓ), projected width (ℓ_o), angle of inclination (β), and surface distance (s) describing LOF test piece defects

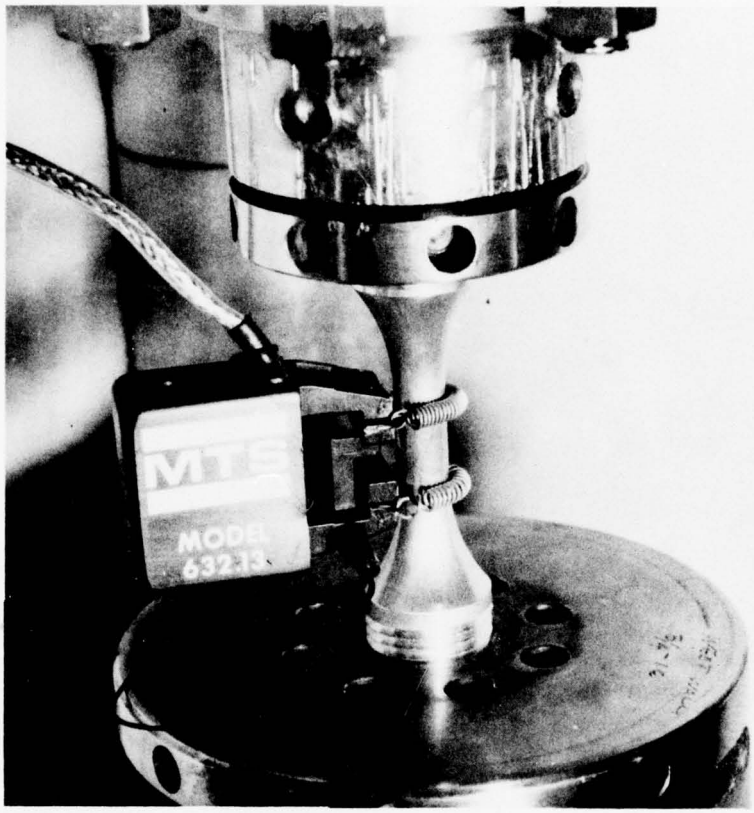

Fig. 5 Strain-control 5083 base metal fatigue specimen with attached extensometer in testing apparatus

P1-2-2-5 (small) ΔS = 12 ksi (82.7 MPa) $2c_o$ = 0.06-in. (1.52 mm) N_f = 413,920

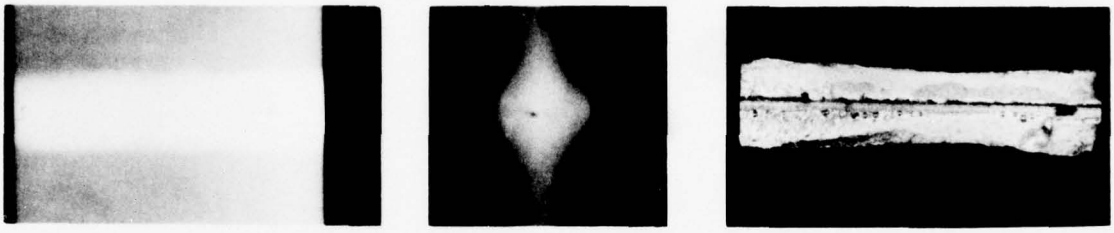

P1-3-1-2 (medium) ΔS = 19 ksi (131.0 MPa) $2c_o$ = 0.08-in. (2.03 mm) N_f = 14,050

P1-4-3-6 (large) ΔS = 12 ksi (82.7 MPa) $2c_o$ = 0.08-in. (2.03 mm) N_f = 133,880

Fig. 6 Test piece fracture surface with edge and normal incidence radiographs for typical small, medium and large LOP defects in 3/8-in. (9.6-mm) thick 5083/5183 Aluminum welds

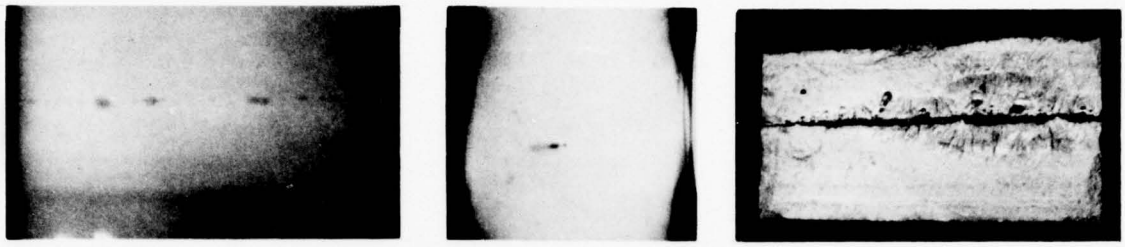

P1-2-2-5 (small) ΔS = 12 ksi (82.7 MPa) $2c_o$ = 0.17-in. (4.32 mm) N_f = 292,610

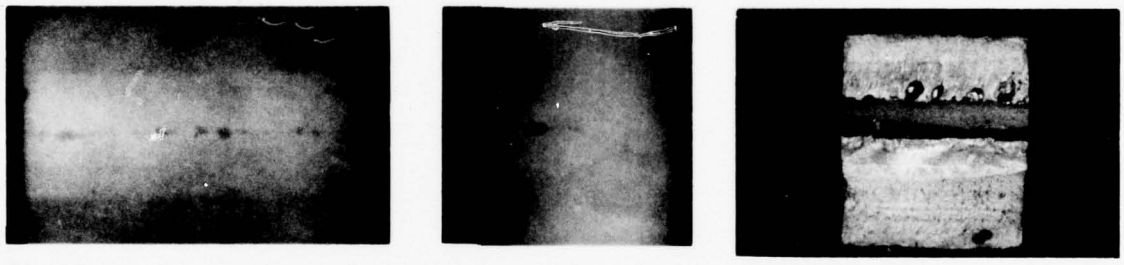

P1-3-1-4 (medium) ΔS = 19 ksi (131.0 MPa) $2c_o$ = 0.24-in. (6.10 mm) N_f = 3,830

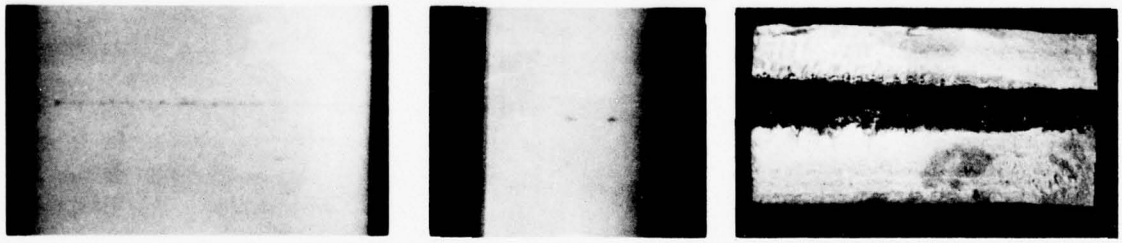

P2-4-3-6 (large) ΔS = 12 ksi (82.7 MPa) $2c_o$ = 0.30-in. (7.62 mm) N_f = 40,850

Fig. 7 Test piece fracture surface with edge and normal incidence radiographs for typical small, medium, and large LOP defects in 1-in. (25-mm) thick 5083/5183 Aluminum welds

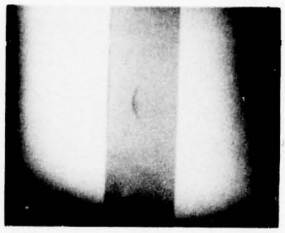

P3-1-1 ΔS = 19 ksi (131.0 MPa) N_f = 46,070
ℓ_o = 0.08-in. (2.03 mm)

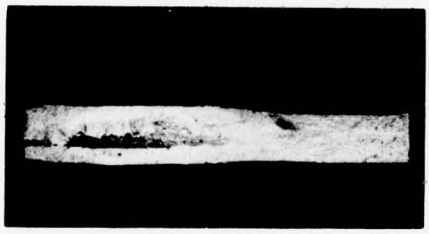

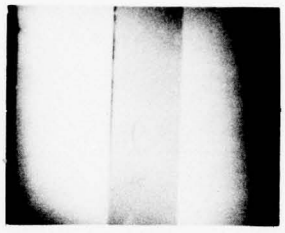

P3-1-2 ΔS = 19 ksi (131.0 MPa) N_f = 34,970
ℓ_o = 0.07-in. (1.78 mm)

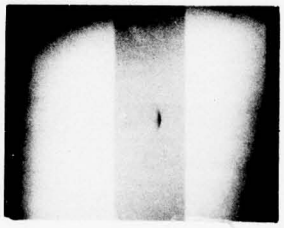

P3-2-10 ΔS = 12 ksi (82.7 MPa) N_f = 1,040,590

Fig. 8 Test piece fracture surface and edge shot radiograph of typical intermittent LOF defects in 3/8-in. (9.6-mm) thick 5083/5183 Aluminum welds.

P3-3-6 ΔS = 12 ksi (82.7 MPa) N_f = 1,222,010
ℓ_o = 0.30-in. (7.62 mm)

P3-3-7 ΔS = 12 ksi (82.7 MPa) N_f = 222,830
ℓ_o = 0.12-in. (3.05 mm)

P3-3-8 ΔS = 12 ksi (82.7 MPa) N_f = 407,180
ℓ_o = 0.10-in. (2.54 mm)

Fig. 9 Test piece fracture surface and edge shot radiograph of typical intermittent LOF defects in 1-in. (25-mm) thick 5083/5183 Aluminum welds

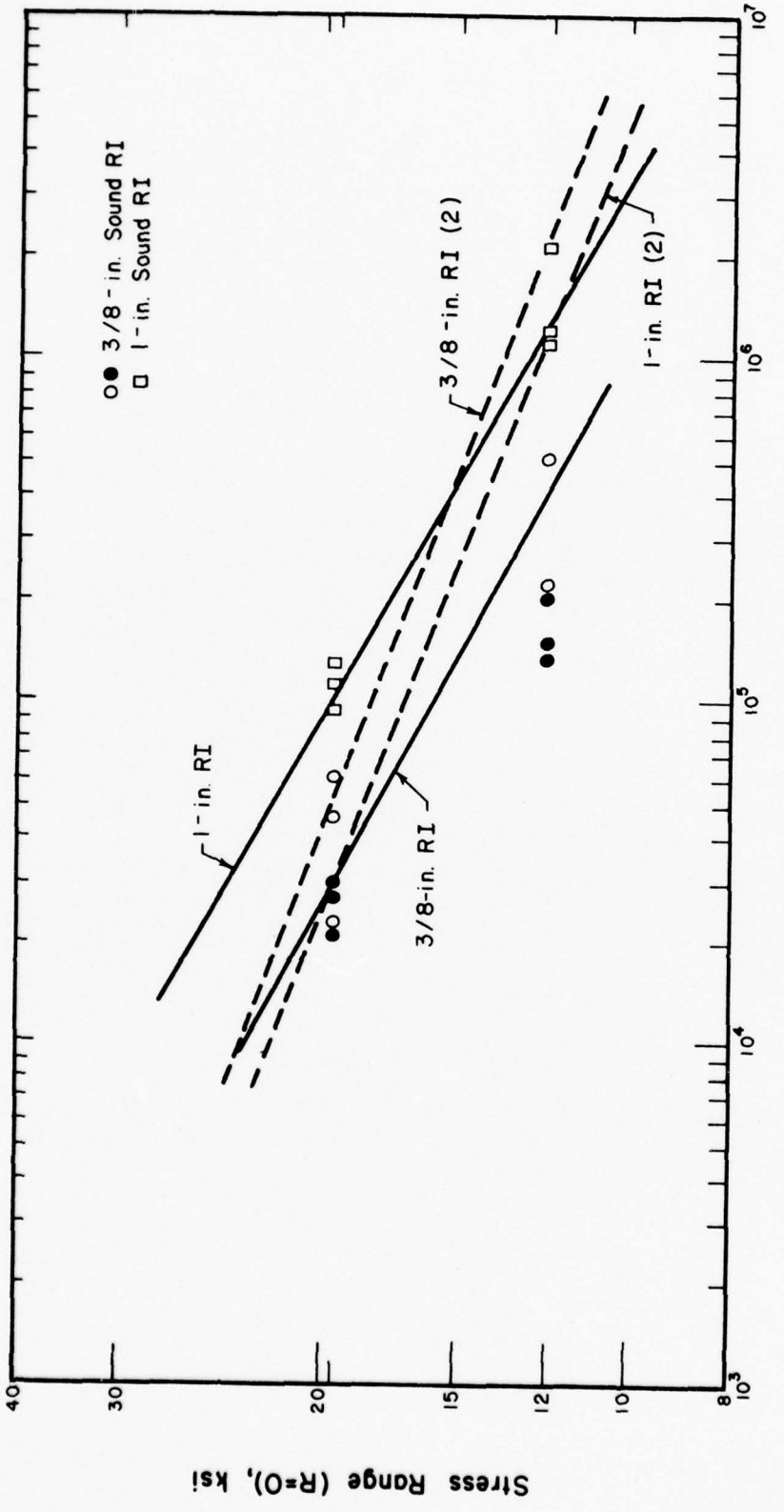

Fig. 10 S-N diagram for sound weld RI fatigue tests with best-fit dashed lines computed using the open symbols. Solid lines represent results from a prior study (Ref. 2) for sound RI 5083/5183 welds

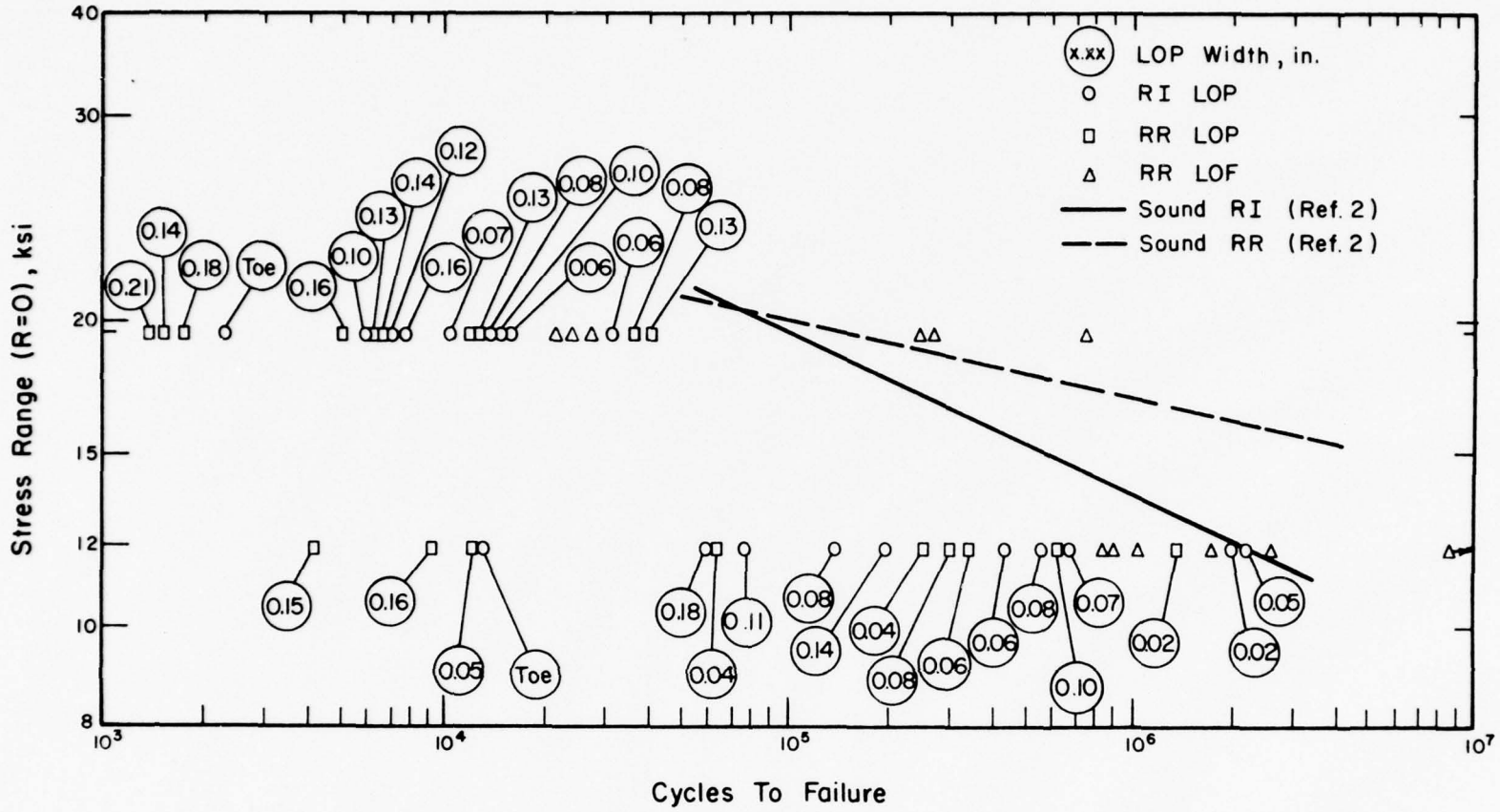

Fig. 11 S-N Diagram for 3/8-in. (9.6-mm) RI and RR test pieces with LOP and LOF defects. The LOP defect length ($2c_0$) is noted in the figure. Results for sound RI and RR welds (Ref. 2) are also plotted

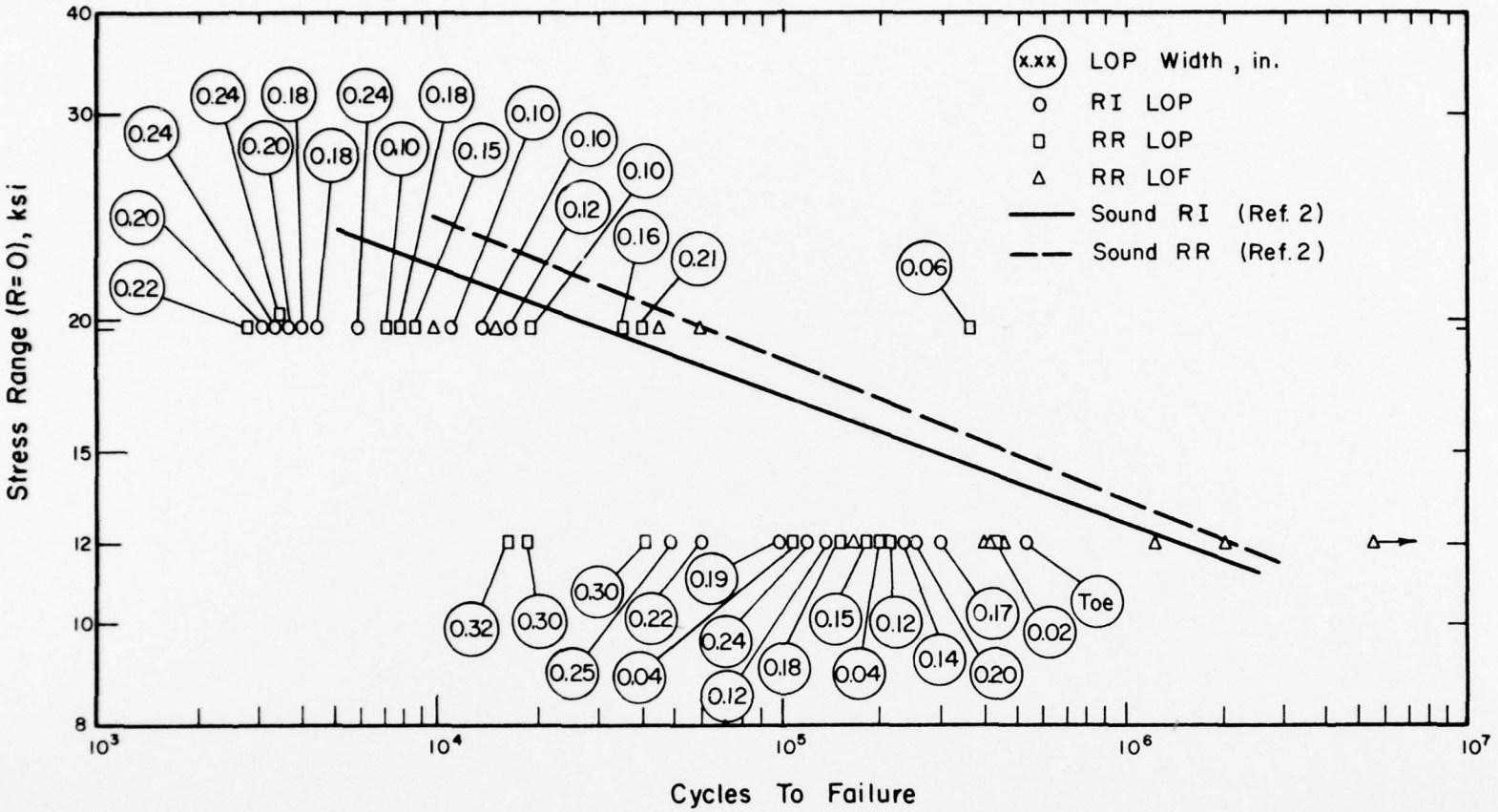

Fig. 12 S-N Diagram for 1-in. (25.4-mm) RI and RR test pieces with LOP and LOF defects. The LOP defect length ($2c_0$) is noted in the figure. Results for sound RI and RR welds (Ref. 2) are also plotted

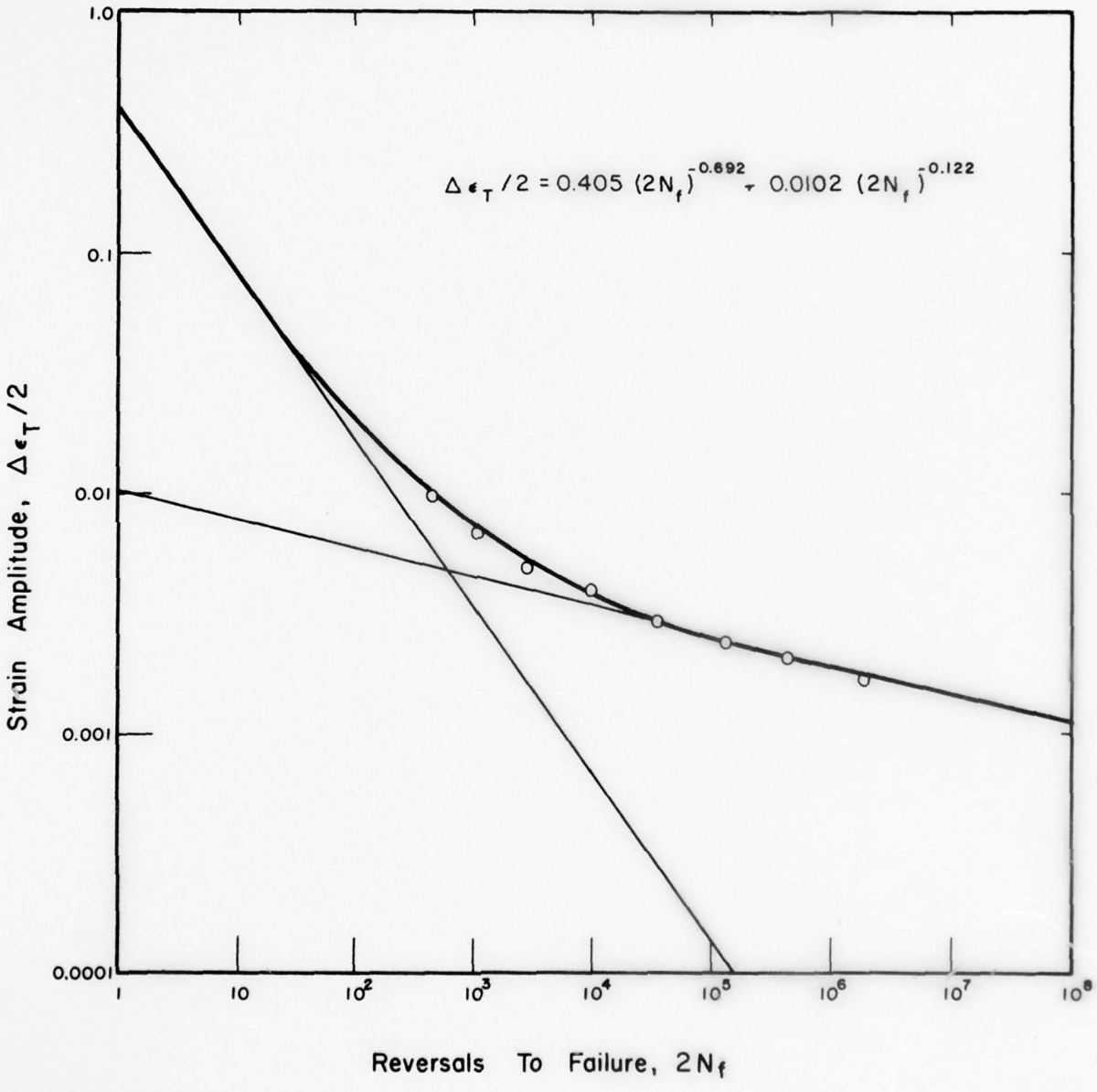

Fig. 13 Strain-life plot for 5083-0 Aluminum base metal for smooth specimens tested under completely reversed (R = - 1) strain control. (Note that 2 reversals = 1 cycle.)

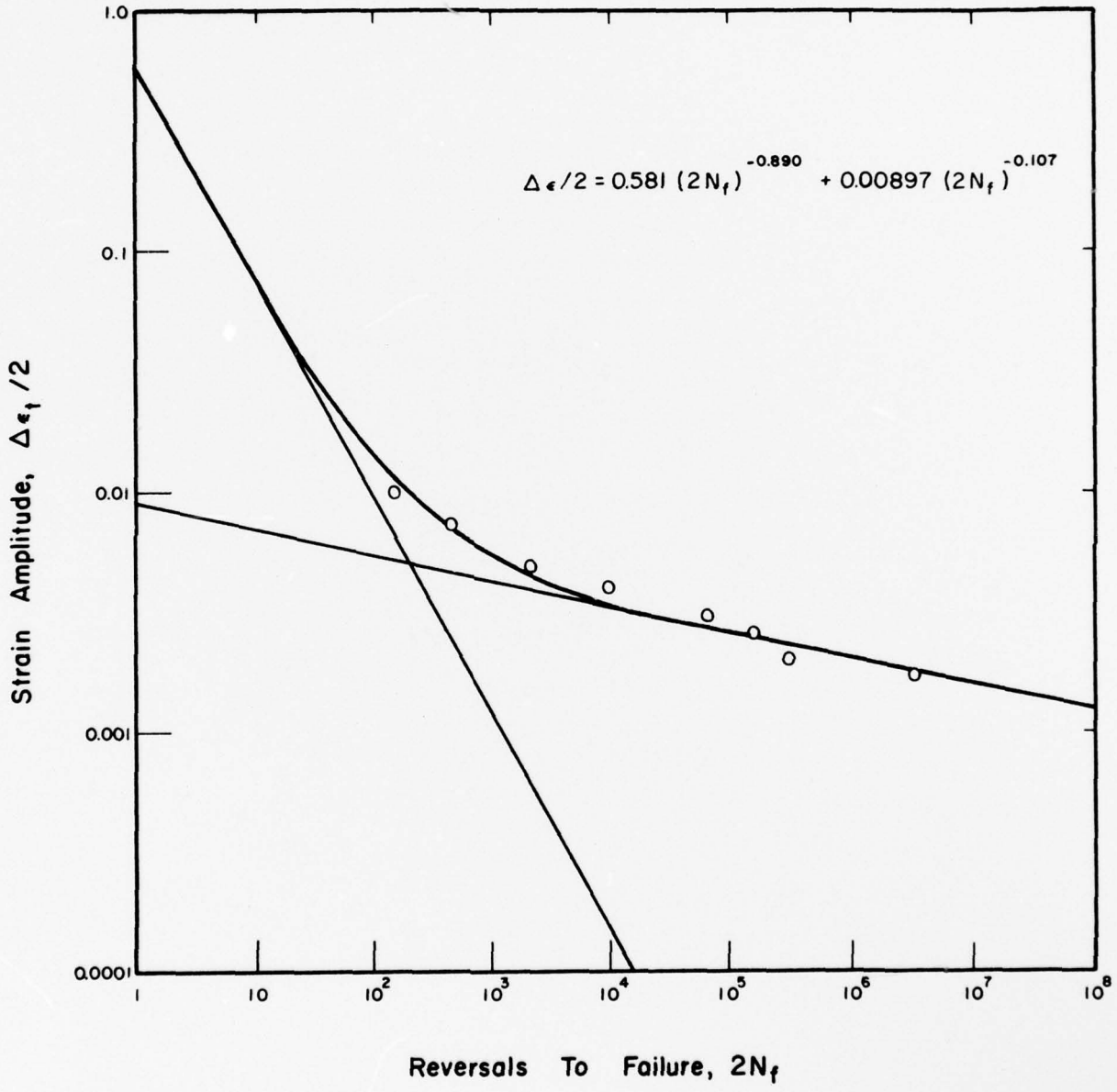

Fig. 14 Strain-life plot for 5183 Aluminum weld metal for smooth specimens tested under completely reversed (R = - 1) strain control.

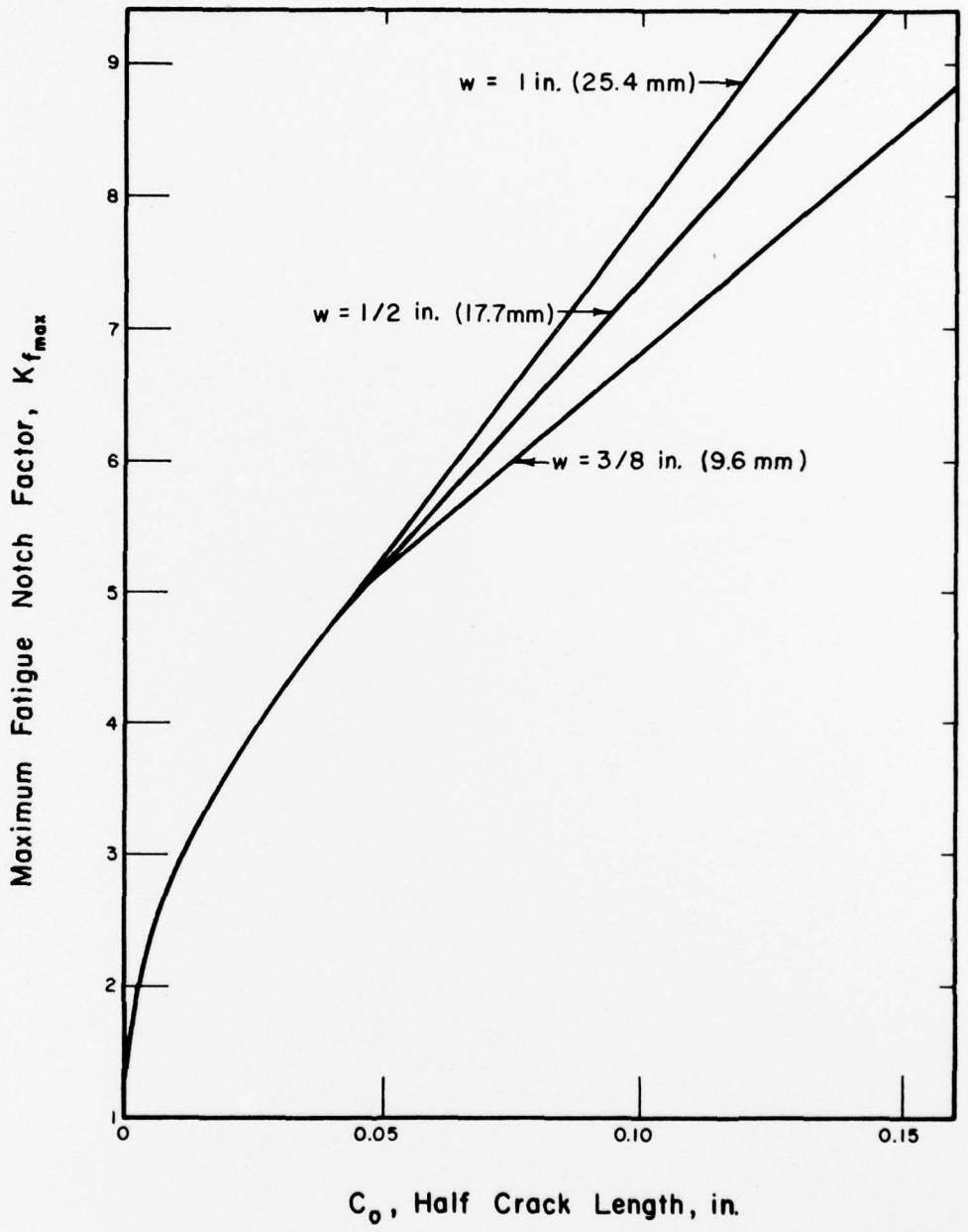

Fig. 15 The relationship between the maximum fatigue notch factor ($K_{f\ max}$) and the half-length (c_o) of the LOP defect for various plate thicknesses. The material constant (a) in Peterson's equation was taken as 0.003-in. (0.076-mm)

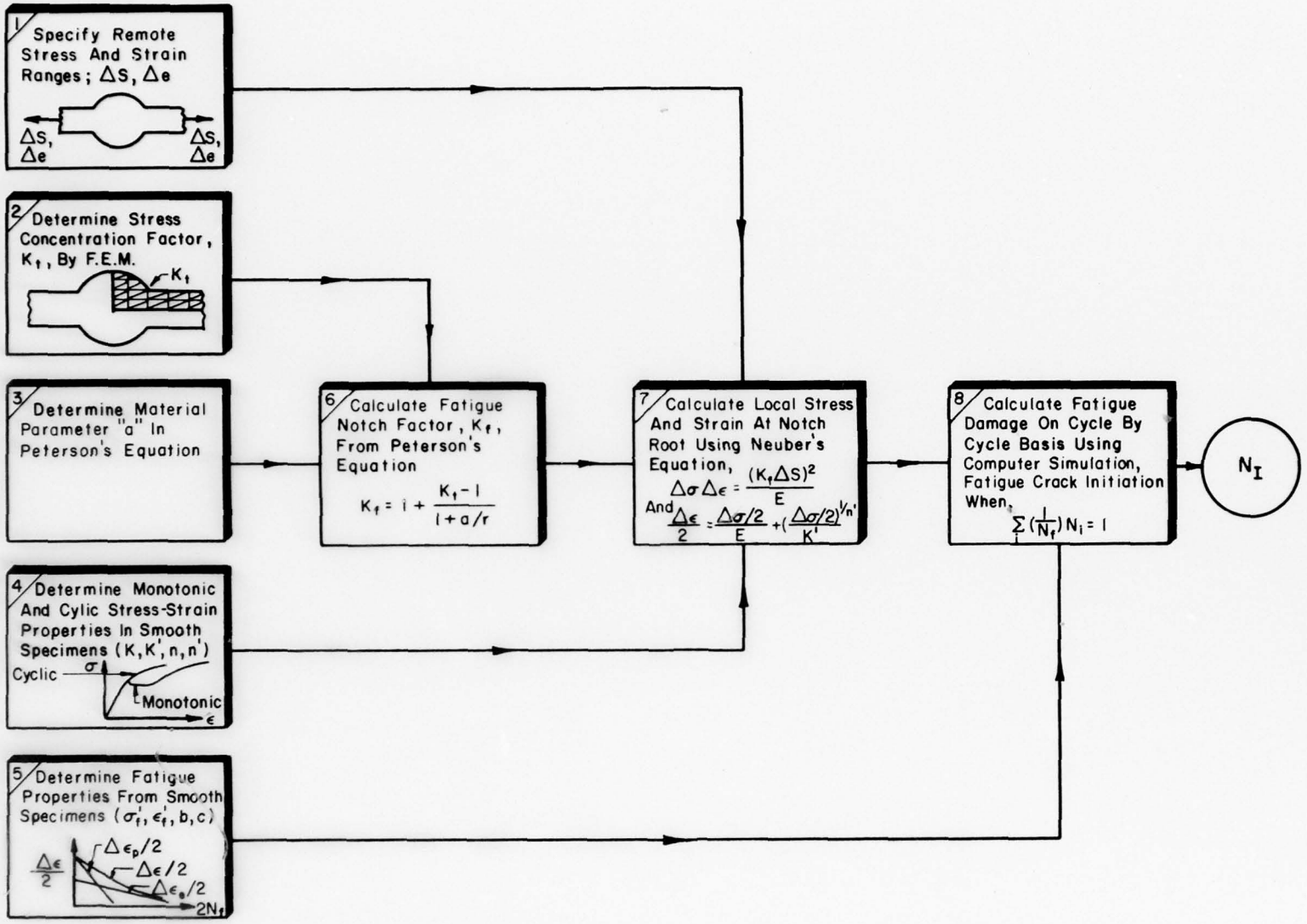

Fig. 16 Steps required for computer simulation of fatigue crack initiation of welds. Steps 1 and 2 require stress analysis results; steps 3 through 5 require the determination of material properties; steps 7 and 8 constitute the computer calculation of damage.

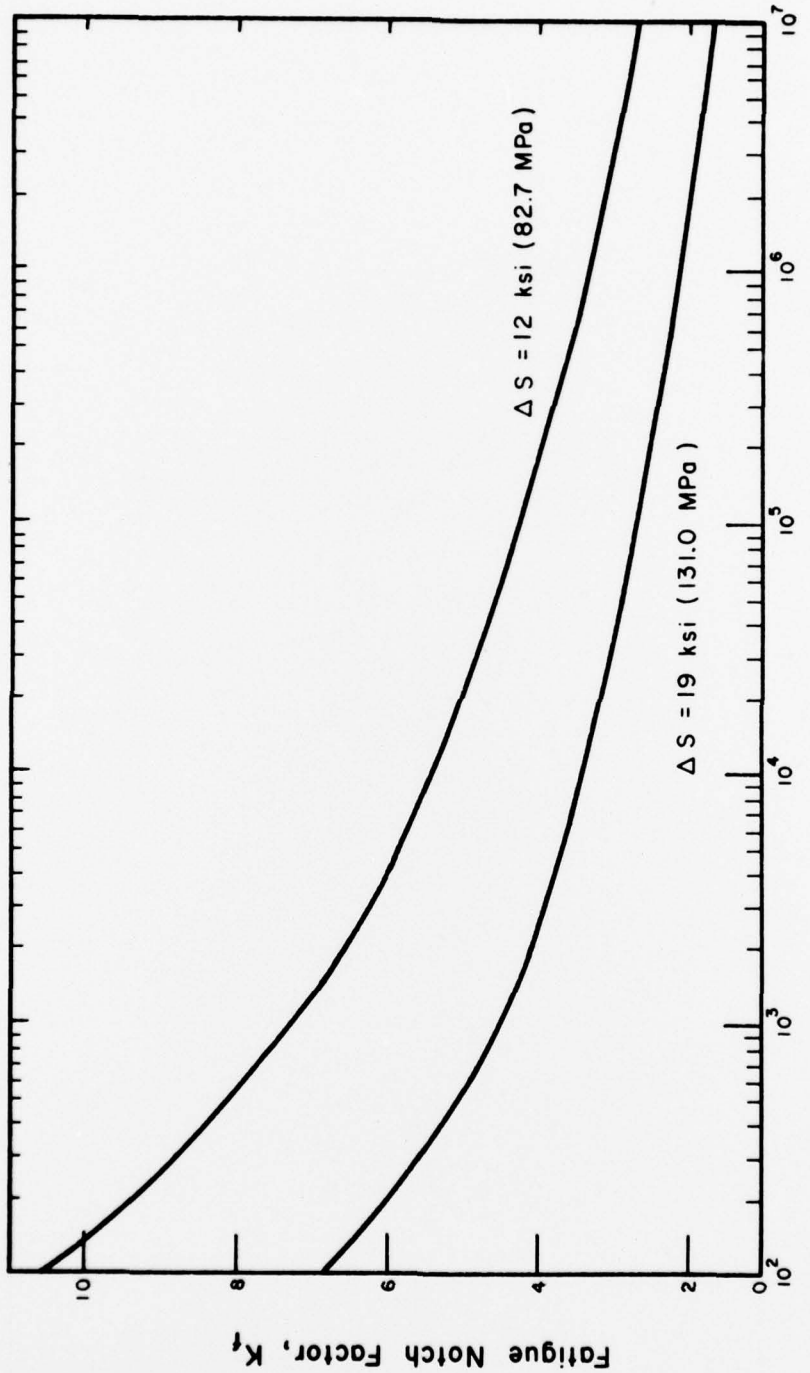

Fig. 17 The relationship between the fatigue notch factor (K_f) and the number of cycles to initiate a crack in 5183 weld metal.

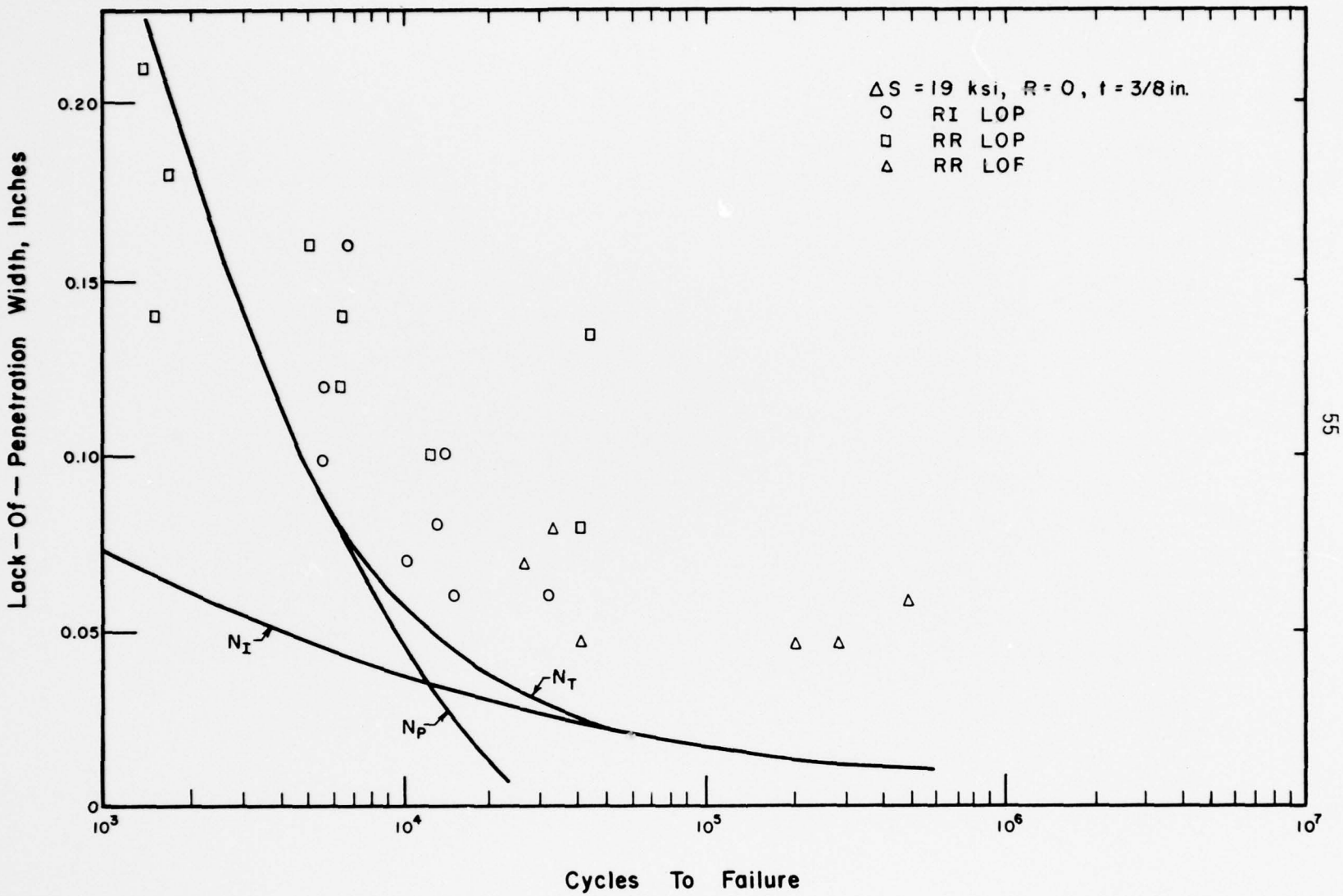

Fig. 18 LOP and LOF width vs. fatigue life for 3/8-in. (9.6-mm) thick RI and RR welds tested at ΔS = 19 ksi (131.0 MPa). The solid lines correspond to the calculated fatigue crack initiation (N_I), fatigue crack propagation (N_p), and the total fatigue life ($N_T = N_I + N_p$).

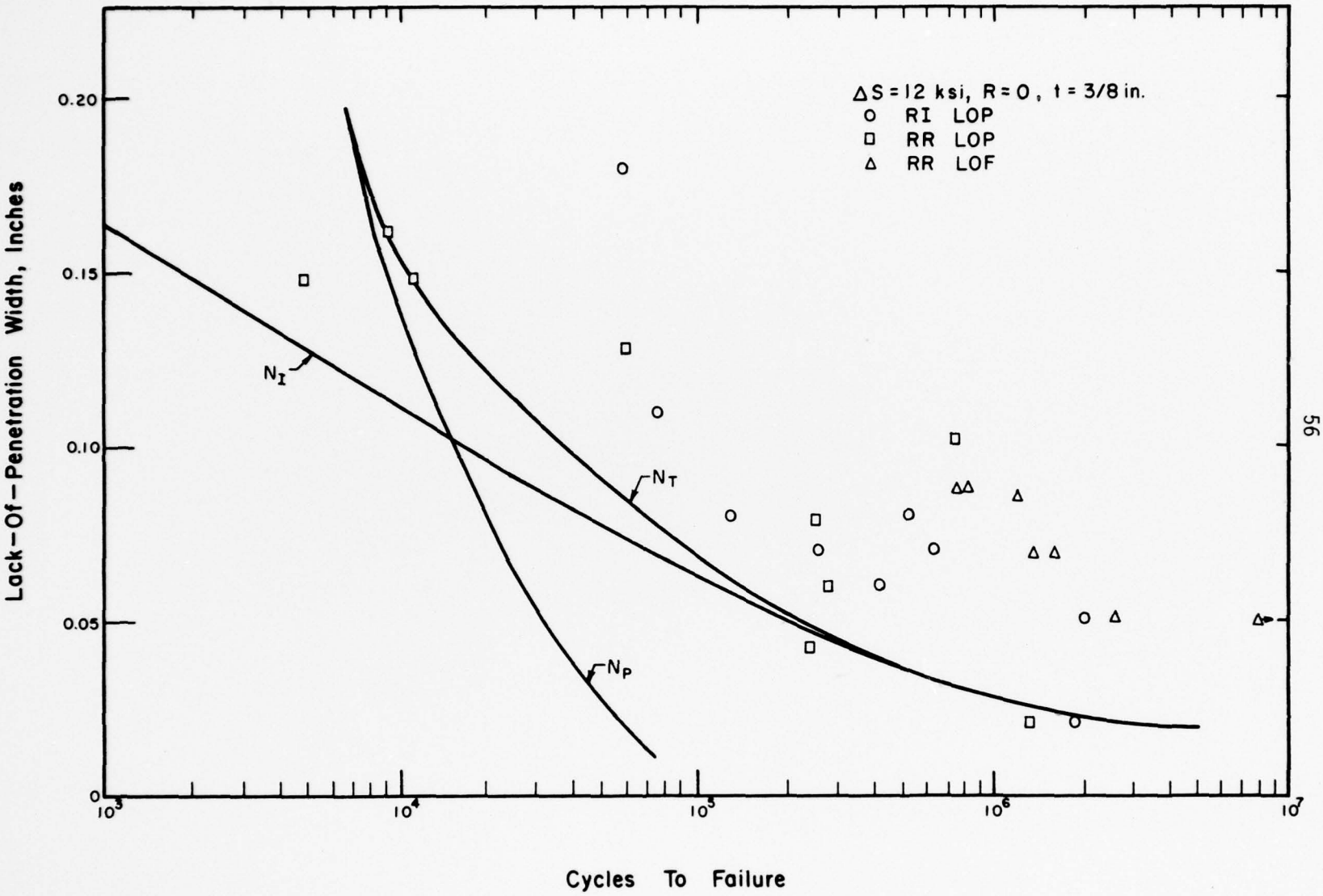

Fig. 19 LOP and LOF width vs. fatigue life for 3/8-in. (9.6-mm) thick RI and RR welds tested at ΔS = 12 ksi (82.7 MPa). The solid lines correspond to the calculated fatigue crack initiation (N_I), fatigue crack propagation (N_p), and the total fatigue life ($N_T = N_I + N_p$).

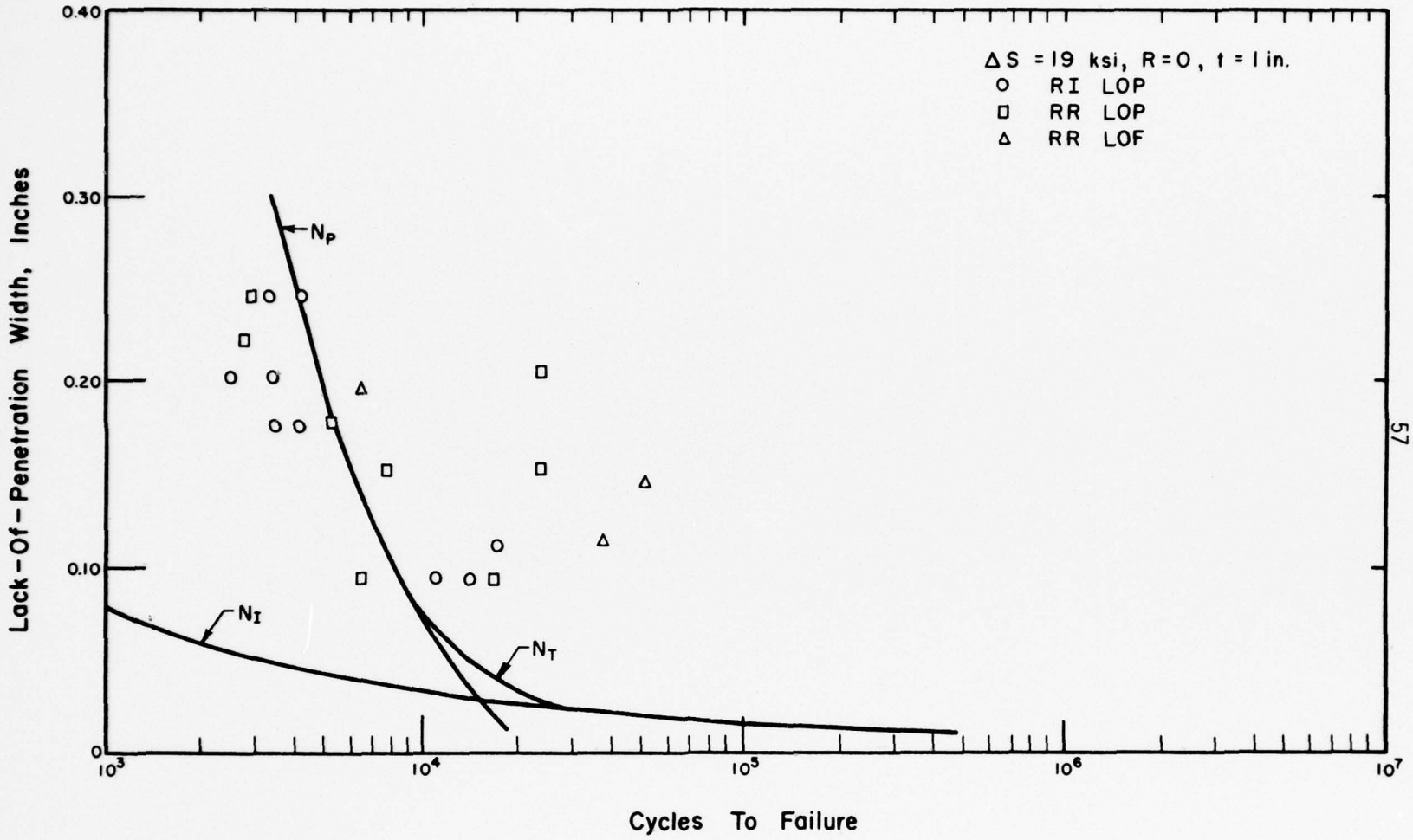

Fig. 20 LOP and LOF width vs. fatigue life for 1-in. (25.4-mm) thick RI and RR welds tested at ΔS = 19 ksi (131.0 MPa). The solid lines correspond to the calculated fatigue crack initiation (N_I), fatigue crack propagation (N_p), and the total fatigue life ($N_T = N_I + N_p$).

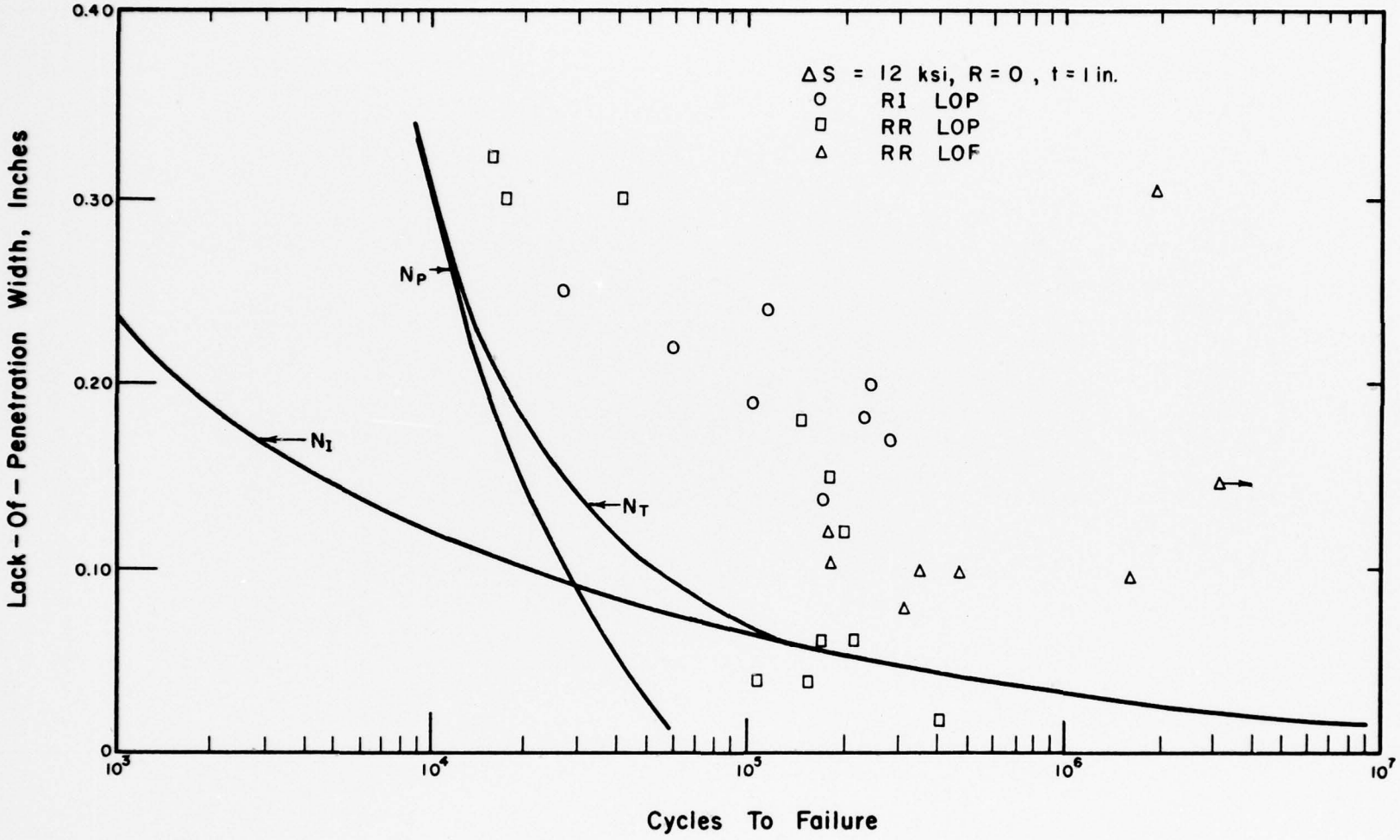

Fig. 21 LOP and LOF width vs. fatigue life for 1-in. (25.4-mm) thick RI and RR welds tested at ΔS = 12 ksi (82.7 MPa). The solid lines correspond to the calculated fatigue crack initiation (N_I), fatigue crack propagation (N_p), and the total fatigue life ($N_T = N_I + N_p$).

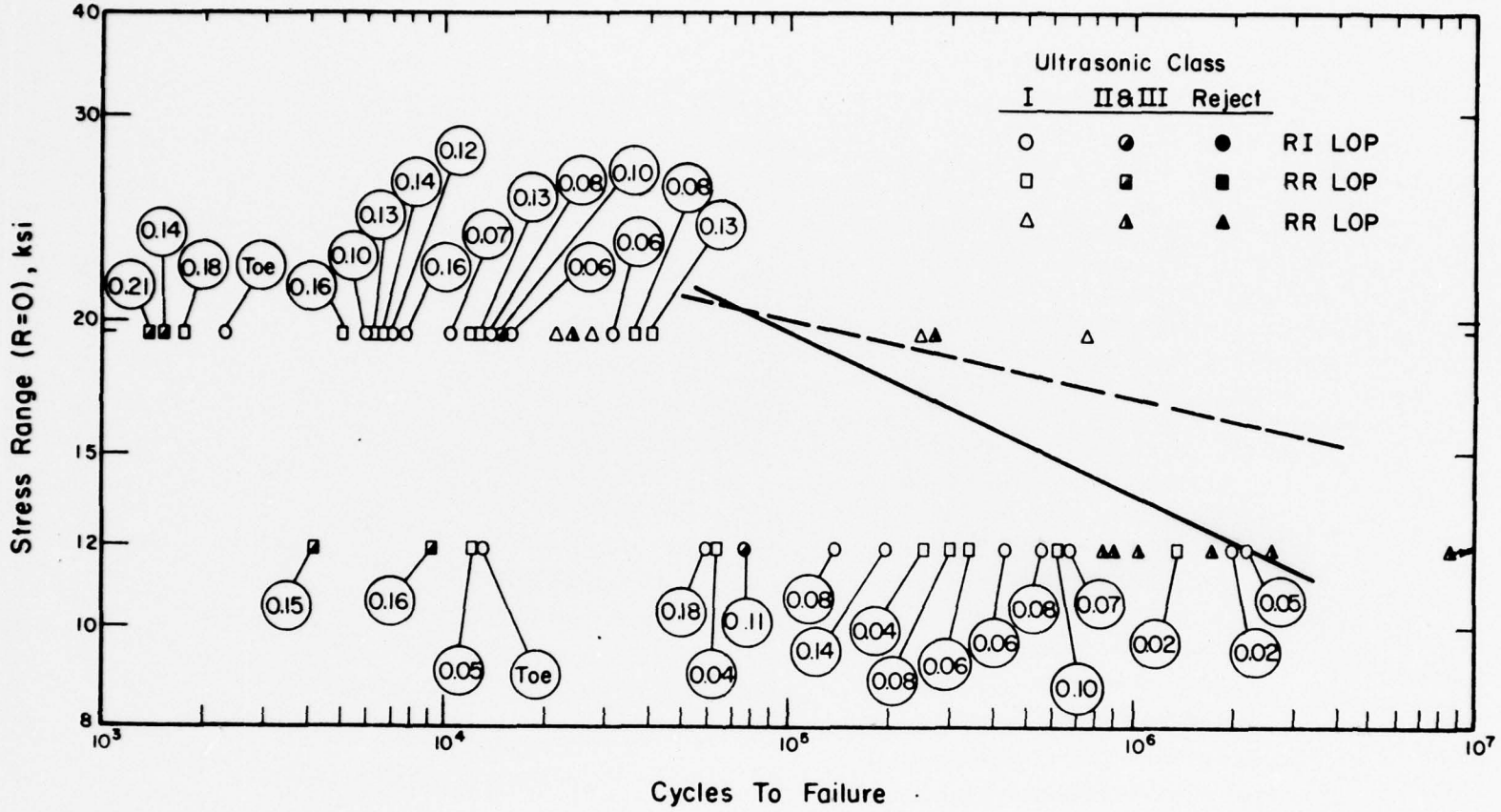

Fig. 22 S-N Diagram for 3/8-in. (9.6-mm) RI and RR test pieces with LOP and LOF defects denoting results of ultrasonic ratings.

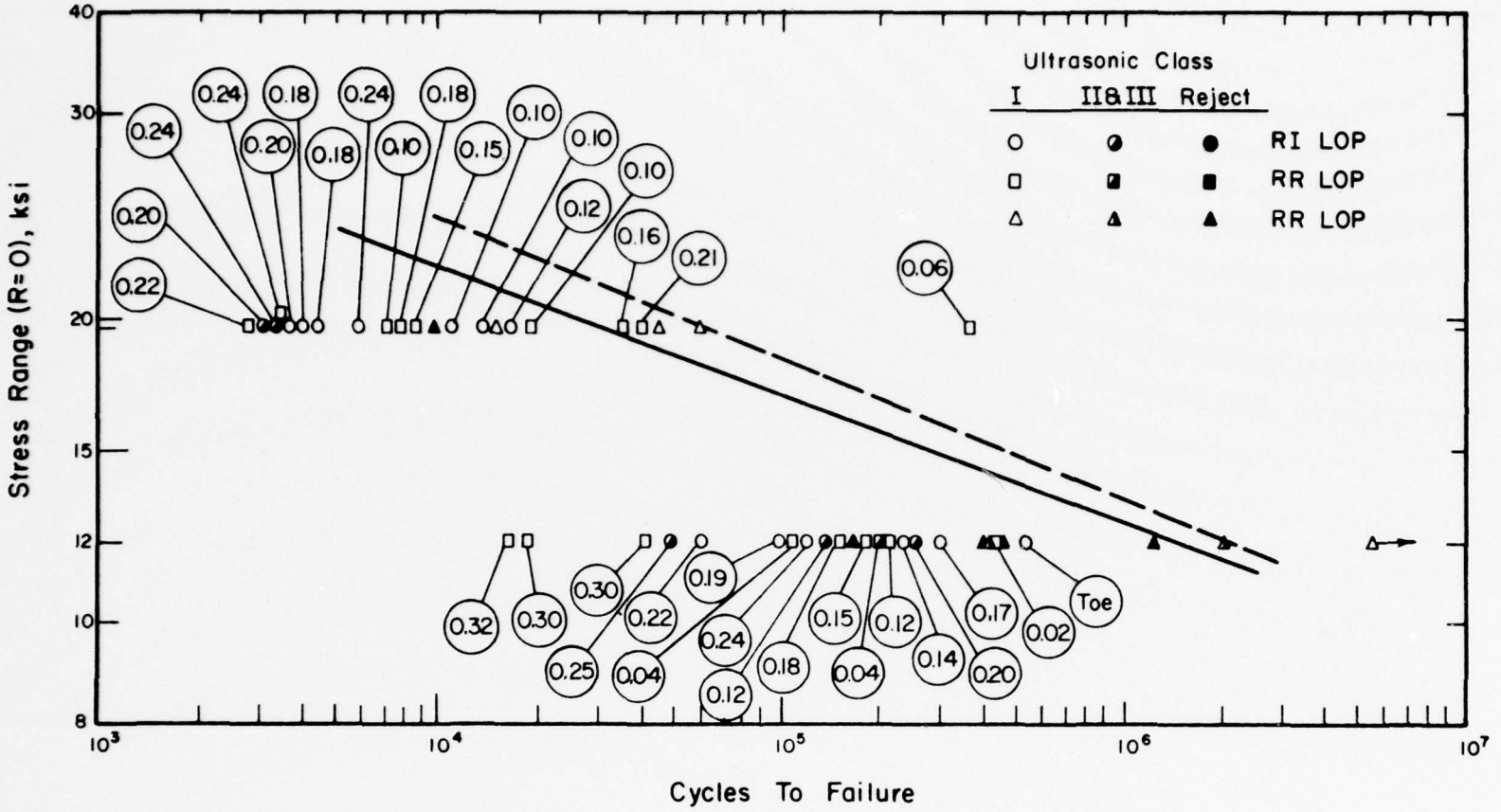

Fig. 23 S-N Diagram for 1-in. (25.4-mm) RI and RR test pieces with LOP and LOF defects denoting results of ultrasonic ratings.

Appendix A

Code Controlling Permissible LOP and LOF Defects for Ultransonic NDT

NAVSHIPS 0900 - 006 - 3010 (January 1966) Ultrasonic Inspection Procedure and Acceptance Standards for Hull Structure Production and Repair Welds

Section 6 Ultrasonic Inspection Procedure Requirements

6.3.4 Reference Calibration Standards

6.3.4.1 The calibration standards for the equipment sensitivity shall be capable of providing constant reference sensitivity levels for all angles of search and inspection depth. The standard reflecting surface shall be a 3/64-in. diameter hole drilled through a 1-1/4 in. wide block. The test surface of the block shall be approximately 250 r.m.s. or compared to surface finish standards.

6.3.5 Calibration

6.3.5.1 When a calibrated decibel control is used, the instrument gain shall be adjusted to peak all signals from the reference clibration holes at 20% of full screen height. The corresponding depth and location of the peaked signals from the reference calibration standard shall be worked along the base line of the viewing screen. The gain shall be increased 12 decibels. At this gain setting, the 20% line on the viewing screen is the DRL (Disregard Level), and the ARL (Amplitude Rejection Level) is 12 decibels above this line. For evaluation of indications above this DRL, the calibrated decibel control is used.

Section 7 Acceptance - Rejection Criteria

7.3.1 Full Penetration Butt Welds and Corner Welds (Class I)

7.3.1.1 Any discontinuity whose reflection exceeds the ARL shall be rejected.

7.3.1.2 Indications less than the DRL shall be disregarded.

7.3.1.3 Discontinuities whose relections equal the DRL, or are greater, up to and including the ARL, shall be evaluated as follows:

a. If the discontinuity length exceeds 1/2t (t=thickness of the thinner member) it shall be rejected. In no case shall any single discontinuity length exceed 1-1/2 inches.

b. Adjacent discontinuities separated by less than 2L of sound metal (L=Length of longest discontinuity) shall be considered as a single discontinuity. The maximum distance between the outer extremities of any two such discontinuities or the sum of their lengths, whichever is greater, shall not exceed the sum of their length specified in 7.3.1.3 (a).

c. If the total accumulative length of discontinuities in any 12 inches of weld length exceeds it, that weld length shall be rejected.

7.3.2 Full Penetration Butt Welds and Corner Welds (Class II)

7.3.3.1 Any discontinuity whose reflection exceeds the ARL and has a length which exceeds 1/2" shall be rejected. Adjacent discontinuities whose reflections exceed the ARL, separated by less than 2L of sound metal L=length of longest discontinuity, shall be considered as a single discontinuity.

7.3.3.2 Indications less than the DRL shall be disregarded. for class III, the DRL shall be increased from 20% to 40% of full screen height.

7.3.3.3 Discontinuities whose reflections equal the DRL, or are greater, up to and including the ARL, shall be rejected if the discontinuity length exceeds 1" or 1t, whichever is greater (t=thickness of the thinner member).

7.3.3.4 Adjacent discontinuities separated by less than 2 L of sound metal, (L=length of longest discontinuity) shall be considered as a single discontinuity. The maximum distance between the outer extremities of any two such adjacent discontinuities or the sum of their lengths, whichever is greater, shall not exceed the length specified in 7.3.3.1 for discontinuities having reflections above the ARL, or 7.3.3.3 for discontinuities having reflections equal to the DRL, up to and including the ARL.

7.3.3.5 If the total accumulative length of discontinuities in any 12 inches of weld length exceeds 2t, that weld length shall be rejected.

APPENDIX B

Code Controlling Permissible LOP and LOF Defects for Radiograph NDT

NAVSHIPS 0900 - 003 - 9000 (March 1967) Radiographic Standards for Production and Repair Welds

3.2 Class I Acceptance Standard for Welds

3.2.2 Incomplete Fusion and Incomplete Penetration Welds Shall be free of incomplete fusion and incomplete penetration indications which exceed the limits of Figure B-1. Acceptable incomplete fusion and incomplete penetration shall be treated as slag when determining the total accummulated length of slag.

3.3 Class II Acceptance Standards for Welds

3.3.2 Incomplete Fusion and Incomplete Penetration shall be free of incomplete fusion and incomplete penetration indications which exceed the limits of Figure B-2. Acceptable incomplete fusion and incomplete penetration shall be treated as slag when determining the total accummulated length of slag.

3.4 Class III Acceptance Standards for Welds

3.4.2 Incomplete Fusion and Incomplete Penetration Welds shall be free of incomplete fusion and incomplete penetration indications which exceed the limits of Figure B-2 Acceptable incomplete fusion and incomplete penetration shall be treated as slag when determining the total accummulated length of slag.

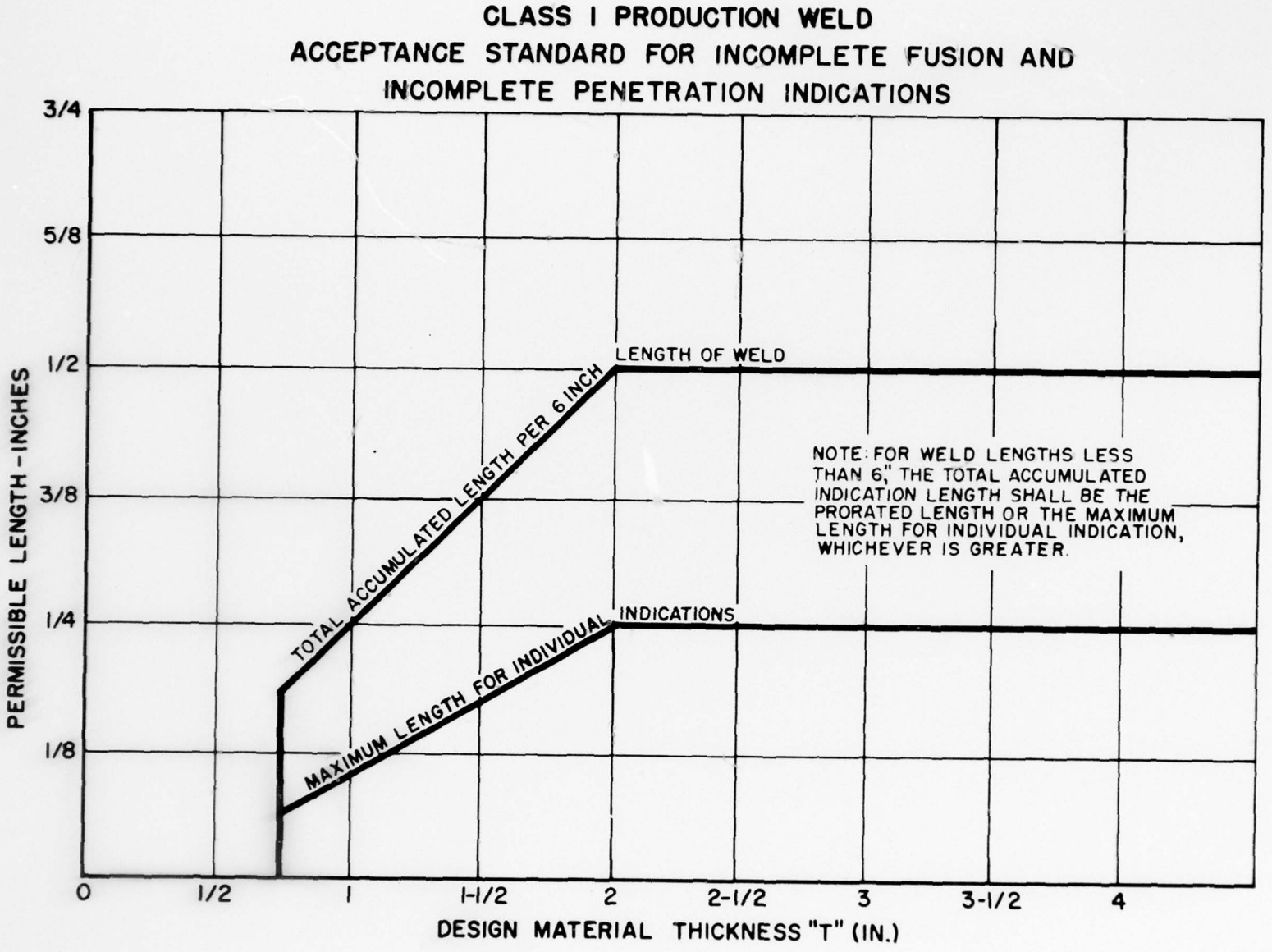
CLASS I PRODUCTION WELD
ACCEPTANCE STANDARD FOR INCOMPLETE FUSION AND
INCOMPLETE PENETRATION INDICATIONS
PERMISSIBLE LENGTH - INCHES
3/4
5/8
1/2
3/8
1/4
1/8
LENGTH OF WELD
TOTAL ACCUMULATED LENGTH PER 6 INCH
MAXIMUM LENGTH FOR INDIVIDUAL INDICATIONS
NOTE: FOR WELD LENGTHS LESS THAN 6," THE TOTAL ACCUMULATED INDICATION LENGTH SHALL BE THE PRORATED LENGTH OR THE MAXIMUM LENGTH FOR INDIVIDUAL INDICATION, WHICHEVER IS GREATER.
0
1/2
1
1-1/2
2
2-1/2
3
3-1/2
4
DESIGN MATERIAL THICKNESS "T" (IN.)

Fig. B-1

CLASS 2 AND 3 PRODUCTION WELD ACCEPTANCE STANDARD FOR INCOMPLETE FUSION AND INCOMPLETE PENETRATION INDICATIONS

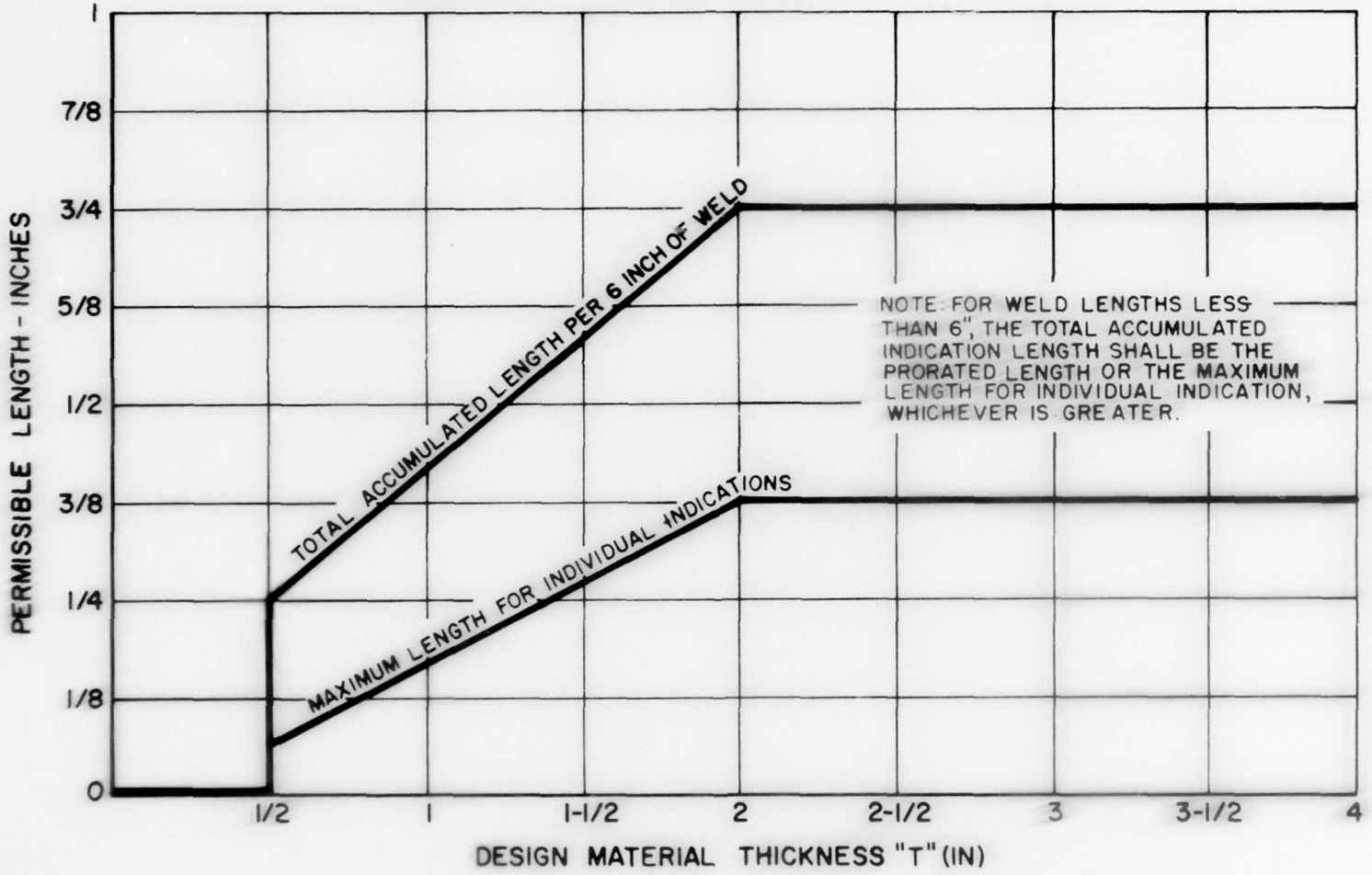

Fig. B-2